Mathematics

https://www.aimspress.com/journal/Math

AIMS Mathematics, 11(9): 29529–29559.
DOI:10.3934/math.20261172
Received: 01 July 2026
Revised: 20 August 2026
Accepted: 26 August 2026
Published: 14 September 2026

Research article

Energy-efficient intermittent control for cluster synchronization of discrete space–time stochastic retarded inertial neural networks

Dong Pan[1,*] **and Shaobin Rao**[2]

[1] School of Basic Science, Guilin University of Technology at Nanning, Nanning 530001, Guangxi, China

[2] Applied Technology College of Soochow University, Suzhou 215325, China

* **Correspondence:** Email: mathsdpan@163.com.

Abstract: This paper investigates mean-square cluster synchronization of discrete-time stochastic inertial neural networks with spatial diffusion, time-varying delays, and stochastic perturbations. A clustered drive–response framework is established via finite-difference approximation and Euler–Maruyama discretization. An intermittent boundary controller is proposed, acting only on boundary nodes for β steps within each period of length θ, thereby reducing the duty ratio from 100% to β/θ. A six-component space–time discrete Lyapunov–Krasovskii functional is constructed, from which interval-dependent matrix-inequality conditions are derived for the control-active and control-inactive intervals. A periodwise contraction condition further links the two regimes and guarantees mean-square exponential cluster synchronization with an explicit convergence rate. Numerical simulations verify the effectiveness of the proposed scheme.

Keywords: cluster synchronization; intermittent boundary control; stochastic inertial neural networks; distributed parameter systems; networked control systems; mean-square exponential stability
Mathematics Subject Classification: 34D06, 34K20, 92B20

1. Introduction

Inertial neural networks (INNs) have attracted sustained attention in recent years because they provide an effective modeling framework for nonlinear systems with acceleration effects, memory dependence, and second-order dynamical characteristics [1–4]. Different from traditional first-order neural network models, INNs contain inertial terms that are closely related to Newtonian mechanics and second-order control systems. More broadly, second-order dynamical structures have also been exploited in continuous-time optimization, where appropriately designed time-varying second-order dynamics can accelerate convergence to optimal solutions [5]. This feature enables INNs to describe oscillatory responses, transient overshoots, and momentum-driven evolution in a more realistic manner. From the viewpoint of systems and control, such models are particularly relevant to large-scale interconnected systems [6–9], where energy exchange, propagation effects, and dynamic coupling play essential roles in the evolution and regulation of network dynamics.

In practical control environments, neural networks [10–13] are usually affected by time delays, spatial propagation, and random disturbances [14–17]. Robustness against external perturbations has also become an important issue in modern neural-network research, including the study of robust adversarial examples for deep neural networks [18]. Time delays [19–21] may arise from finite transmission speeds, signal processing lags, and communication constraints, and spatial diffusion characterizes local interactions among distributed nodes and stochastic perturbations reflect environmental fluctuations or measurement noise [22–24]. When these factors coexist with inertial dynamics [25], the resulting networks exhibit higher-order structures, memory-dependent evolution, spatially distributed coupling, and stochastic uncertainties simultaneously [26]. The interaction among inertia, delay, diffusion, and randomness may lead to oscillation, instability, or complex transient behaviors, which makes the analysis and control synthesis of such systems considerably more challenging.

In many real-world networked systems, synchronization of all nodes is neither necessary nor consistent with the intrinsic heterogeneous structure of the network [27–29]. Related synchronization and control issues have also been studied [30–32]. Cluster synchronization provides a more flexible and practically meaningful coordination mechanism, in which nodes within the same subgroup are required to synchronize, whereas different clusters are allowed to preserve distinct dynamical behaviors [33, 34]. This type of synchronization is closely related to cooperative control problems in heterogeneous multiagent systems, distributed sensor networks, and large-scale neural structures. Although cluster synchronization has been widely investigated for deterministic or first-order systems, the corresponding control and analysis problems for stochastic inertial neural networks (SINNs) with clustered architectures remain far from complete, especially when discrete space–time dynamics are involved.

To facilitate digital implementation and numerical simulation while preserving spatial propagation and stochastic effects [14–17], continuous reaction–diffusion INNs are often converted into discrete space–time models. Finite-difference schemes are used to approximate spatial diffusion operators, and stochastic discretization methods, such as the Euler–Maruyama approach [35], are employed to characterize random perturbations. This procedure leads to discrete space–time SINNs governed by partial difference equations [7–9]. Compared with continuous-time models, such discrete systems simultaneously involve second-order difference dynamics, delay-dependent nonlinear couplings, spatial diffusion, and stochastic disturbances. These features make mean-square stability analysis and synchronization controller design substantially more difficult. Therefore, developing rigorous discrete-time control criteria for space–time SINNs is of both theoretical importance and practical relevance for networked and distributed parameter systems.

Whereas space–time discretization provides an effective framework for describing diffusion dynamics, stochastic disturbances constitute another important source of uncertainty in practical neural networks [36–38]. Random fluctuations may arise from environmental uncertainty, communication noise, sensor inaccuracies, and external disturbances, and they can significantly affect the synchronization performance of networked systems. In contrast to deterministic networks, stochastic neural networks require synchronization and stability to be investigated in probabilistic or mean-square senses, which introduces additional analytical challenges. Although stochastic synchronization [7, 16, 26] has attracted considerable attention in recent years, existing results mainly focus on continuous-time or first-order models. The corresponding cluster synchronization problem for discrete space–time stochastic inertial neural networks remains far from fully understood, especially in the presence of diffusion coupling and time-varying delays.

Time delays further increase the difficulty of the synchronization problem from both analysis and control perspectives [39–42]. Delay-dependent terms introduce additional memory effects and may interact nontrivially with inertial dynamics and stochastic perturbations. In the stochastic systems [4, 14, 36], delays may appear in both the deterministic drift part and the stochastic diffusion part, which makes mean-square synchronization analysis more challenging than that for deterministic systems. Thus, establishing delay-dependent criteria that guarantee asymptotic and exponential synchronization for discrete SINNs is a meaningful and nontrivial problem in stochastic networked control.

For distributed systems governed by partial differential equations [43], boundary control (BC) provides an effective way to regulate global network dynamics through spatially localized actuation [44]. By applying control inputs only at boundary nodes, BC can reduce implementation cost while affecting the interior states through diffusion coupling. Existing studies on space–time discrete neural networks mainly rely on continuous BC strategies. Compared with internal control, boundary control offers a different trade-off between control performance and implementation cost. Internal control can directly regulate states at spatially distributed locations and may therefore provide faster local control action; however, it generally requires actuators, sensors, and communication channels to be deployed inside the spatial domain, which may increase installation, communication, and maintenance costs, especially for large-scale distributed parameter systems. In contrast, boundary control applies actuation only at accessible boundary locations and influences the interior states through spatial diffusion [42]. This feature makes boundary control physically attractive when internal nodes are difficult, expensive, or impractical to access. Nevertheless, because the control effect must propagate from the boundary into the interior domain, its transient regulation may be less direct than that of internal control. Therefore, boundary control provides a practically meaningful compromise between spatial actuation cost and synchronization performance. However, continuous boundary actuation may lead to unnecessary energy consumption and may be difficult to implement when actuators are subject to duty-cycle, communication, or resource constraints. Intermittent control, in which control inputs are activated only during prescribed time intervals, offers a more flexible and energy-efficient alternative for practical networked and distributed parameter systems. Although intermittent synchronization has been widely studied for deterministic or first-order systems, the corresponding results for discrete space–time SINNs with clustered structures and stochastic perturbations remain scarce.

In light of the above discussions and the limitations of existing studies on discrete SINNs [7–9], this paper develops an intermittent boundary control framework for mean-square cluster synchronization of discrete space–time SINNs. The emphasis is placed not only on the modeling of clustered stochastic inertial dynamics, but also on the design of an energy-efficient boundary controller and the derivation of tractable synchronization criteria. The main contributions are highlighted as follows.

- A clustered drive–response framework is established for discrete space–time SINNs with spatial diffusion, inertial dynamics, time-varying delays, and stochastic perturbations. This framework extends existing studies from single-network stability, boundedness, and periodicity analysis to multigroup cooperative synchronization control.

- An intermittent boundary control strategy is proposed for cluster synchronization. The controller is imposed only on boundary nodes and is activated only during prescribed control intervals. Compared with continuous boundary control, the proposed scheme reduces the control activation time and is more suitable for energy-constrained distributed parameter and networked control systems.

- A six-component space–time discrete Lyapunov–Krasovskii functional is constructed to jointly capture second-order inertial differences, spatial diffusion, stochastic perturbations, and time-varying delays. Different from conventional single-regime linear matrix inequality (LMI)-based stability conditions, the resulting synchronization criterion consists of two coupled matrix-inequality conditions corresponding to the control-active and control-inactive intervals. These conditions are further linked by a periodwise contraction factor that explicitly incorporates the control duty cycle, thereby quantifying how the decay accumulated during the active interval compensates for the possible growth during the inactive interval and yielding an explicit mean-square exponential convergence rate.

These results provide a computationally tractable theoretical basis for the analysis and design of energy-efficient coordinated control schemes for high-dimensional stochastic diffusion neural networks. They also offer a useful control-oriented framework for discrete distributed parameter systems with intermittent actuation, spatial coupling, time delays, and random perturbations.

This paper is structured as follows. Section 2 formulates the discrete space-time SINNs' model with clustering structure and introduces the corresponding drive–response framework. In Section 3, a novel discrete Lyapunov–Krasovskii functional consisting of six components is constructed, and several preliminary lemmas, including Wirtinger-type inequalities, are presented to facilitate the subsequent analysis. Section 3 establishes sufficient criteria for mean-square exponential cluster synchronization of the drive-response systems under intermittent BC, expressed in terms of solvable matrix inequalities. A numerical example in Section 4 is provided to verify the effectiveness of the proposed control strategy and to illustrate the theoretical findings. Finally, Section 5 concludes the paper and outlines possible directions for future research.

Before presenting the model formulation, the notation used throughout this paper is introduced below.

Mathematical symbols and abbreviations: $\mathbb{R}^n$ denotes the n-dimensional Euclidean space equipped with the standard norm $\|\cdot\|$. $\mathbb{Z}$ represents the set of all integers, $\mathbb{Z}_0 = \{0, 1, 2, \ldots\}$, and $\mathbb{Z}_+ = \{1, 2, 3, \ldots\}$. For any subsets $I, J \subseteq \mathbb{R}$, the notation $I \cap J$ denotes their intersection.

For a function $z : \mathbb{Z} \times \mathbb{Z} \to \mathbb{R}^n$, let $z_k^{[\iota]} = (z_{1,k}^{[\iota]}, \ldots, z_{n,k}^{[\iota]})^T$, where ι and k represent the spatial and temporal indices, respectively. The forward difference operator with respect to time is defined as

$$\Delta z_k^{[\iota]} = z_{k+1}^{[\iota]} - z_k^{[\iota]}, \quad \Delta^2 z_k^{[\iota]} = z_{k+2}^{[\iota]} - 2z_{k+1}^{[\iota]} + z_k^{[\iota]}.$$

The spatial forward difference operator is given by $\Delta_\iota z_k^{[\iota]} = (z_k^{[\iota+1]} - z_k^{[\iota]})/\hbar$, and the second-order spatial difference operator is

$$\Delta_\iota^2 z_k^{[\iota]} = \Delta_\iota(\Delta_\iota z_k^{[\iota]}) = \frac{z_k^{[\iota+2]} - 2z_k^{[\iota+1]} + z_k^{[\iota]}}{\hbar^2},$$

where $(\iota, k) \in \mathbb{Z} \times \mathbb{Z}$, and $\hbar > 0$ denotes the spatial step size.

For a square matrix $\mathbf{A} \in \mathbb{R}^{n\times n}$, ddiag($\mathbf{A}$) denotes the diagonal matrix whose diagonal entries coincide with those of $\mathbf{A}$. Throughout the paper, $\mathbf{A} > 0$ ($\mathbf{A} \geq 0$) indicates that the matrix $\mathbf{A}$ is positive definite (positive semidefinite). $\mathbb{E}\{\cdot\}$ denotes the mathematical expectation operator.

2. Clustered differencing SINNs

In this section, we formulate a class of clustered space–time differencing stochastic inertial neural networks (SINNs) that serve as the fundamental model for subsequent synchronization analysis. By employing the forward difference operator and the second-order time difference, the inertial effect of neurons is characterized in a fully discrete-time framework, and a spatial discrete diffusion operator is introduced to describe the local coupling and propagation behavior among neighboring nodes. The resulting model incorporates inertial terms, damping effects, spatial diffusion, deterministic synaptic coupling, stochastic perturbations, and dual time-varying delays appearing in both the drift and diffusion channels. Furthermore, the network nodes are partitioned into multiple clusters, and clusterwise parameter consistency is imposed to reflect structural similarity within each group. Based on this clustered configuration, a drive–response scheme is constructed, which enables the derivation of the associated error dynamics and lays the groundwork for the analysis of mean-square exponential cluster synchronization. The proposed clustered differencing SINN model captures the combined influence of inertia, diffusion, delay, and stochastic disturbances, providing a rigorous mathematical framework for studying synchronization behavior in discrete space–time neural networks. The control objective is to design an intermittent boundary actuation law for the response network such that the synchronization error converges exponentially in the mean-square sense.

The basic network model considered here is developed from the discrete-time and discrete-space stochastic INNs studied in [7–9]. Such models can be obtained from continuous reaction–diffusion INNs by applying finite-difference approximation to the spatial diffusion terms and the Euler–Maruyama scheme [35] to the stochastic dynamics. On this basis, we incorporate time-varying delays and subsequently introduce a clustered drive–response structure for synchronization analysis. Accordingly, the following space–time discrete stochastic INNs are considered:

$$\begin{aligned} \Delta^2 z_{i,k}^{[\iota]} &= 2(e^{-\frac{1}{2}a_i h} - 1)\Delta z_{i,k}^{[\iota]} + \left[\frac{2 - 2e^{-\frac{1}{2}a_i h}}{a_i}\right]^2 \Big[\gamma_i \Delta_\iota^2 z_{i,k}^{[\iota-1]} - b_i z_{i,k}^{[\iota]} \\ &\quad + \sum_{j=1}^{n} c_{ij} f_j(z_{j,\delta_k}^{[\iota]}) + \frac{1}{\sqrt{h}} \sum_{j=1}^{n} \xi_{ij}\sigma_j(z_{j,o_k}^{[\iota]})\varepsilon_{j,k} + I_i\Big], \quad \forall \iota \in (0, \aleph)_{\mathbb{Z}}, \end{aligned} \tag{2.1}$$

where $i = 1, 2, \ldots, n$; the variable z_i denotes the dynamical state associated with neuron i; the parameters a_i and $b_i > 0$ represent the damping coefficient and the intrinsic feedback intensity of neuron i, respectively; the symbol γ_{ip} characterizes the diffusion rate; the coefficients c_{ij} and ξ_{ij} describe the deterministic and stochastic coupling strengths between neurons; the functions $f_j(\cdot)$ and $\sigma_j(\cdot)$ correspond to the activation mapping and the noise intensity function, respectively; the term

I_i accounts for external stimuli applied to neuron i; the positive constants $\hbar$ and h (with $\hbar, h < 1$) denote the spatial and temporal discretization step sizes, respectively; the delay terms δ_k and o_k satisfy $0 \leq \delta_k, o_k \leq \delta_\infty$ for all $k \in \mathbb{Z}_0$, where $\delta_\infty \geq 1$ is a prescribed integer bound; the random variables $\varepsilon_{j,k} \sim \mathcal{N}(0,1)$ are independent standard Gaussian sequences; and $\{\varepsilon_{j,k}\}_{j=1}^n$ are mutually independent for each fixed k. The factor $1/\sqrt{h}$ in the stochastic term arises from the Euler–Maruyama discretization. Indeed, for a Brownian increment over the time step h, one has $\Delta B_{j,k} = \sqrt{h}\,\varepsilon_{j,k}$ with $\varepsilon_{j,k} \sim \mathcal{N}(0,1)$, and hence, $\Delta B_{j,k}/h = \varepsilon_{j,k}/\sqrt{h}$. The initial conditions together with the mixed boundary conditions of System (2.1) are given by

$$\begin{cases} z_{i,\tau}^{[\iota]} = \varphi_{i,\tau}^{[\iota]}, \quad \forall \tau \in [-\delta_\infty, 1]_{\mathbb{Z}}, \iota \in (0, \aleph)_{\mathbb{Z}}; \\ z_{i,k}^{[0]} = 0 = \Delta_\iota z_{i,k}^{[\aleph-1]}, \end{cases} \tag{2.2}$$

$\forall k \in \mathbb{Z}_0, i = 1, 2, \ldots, n$.

Corresponding to the drive system (2.1), the response SINNs are formulated as follows:

$$\begin{cases} \Delta^2 w_{i,k}^{[\iota]} = 2(e^{-\frac{1}{2}a_i h} - 1)\Delta w_{i,k}^{[\iota]} + \left[\dfrac{2 - 2e^{-\frac{1}{2}a_i h}}{a_i}\right]^2 \Big[\gamma_i \Delta_\iota^2 w_{i,k}^{[\iota-1]} - b_i w_{i,k}^{[\iota]} \\ \qquad + \displaystyle\sum_{j=1}^n c_{ij} f_j(w_{j,\delta_k}^{[\iota]}) + \frac{1}{\sqrt{h}} \sum_{j=1}^n \xi_{ij} \sigma_j(w_{j,o_k}^{[\iota]})\varepsilon_{j,k} + I_i\Big], \quad \forall \iota \in (0, \aleph)_{\mathbb{Z}}, \\ w_{i,\tau}^{[\iota]} = \phi_{i,\tau}^{[\iota]}, \quad \forall \tau \in [-\delta_\infty, 1]_{\mathbb{Z}}, \iota \in (0, \aleph)_{\mathbb{Z}}, \\ w_{i,k}^{[0]} = 0, \ \Delta_\iota w_{i,k}^{[\aleph-1]} = \rho_{i,k}, \end{cases} \tag{2.3}$$

where $k \in \mathbb{Z}_0$, $i = 1, 2, \ldots, n$. Here, ρ_i denotes the intermittent control action applied at the boundary, and its specific design will be specified subsequently.

Suppose that the node set $\mathcal{C} := \{1, 2, \ldots, n\}$ is divided into m disjoint subsets $\{\mathcal{C}_1, \mathcal{C}_2, \ldots, \mathcal{C}_m\}$ such that $\mathcal{C} = \bigcup_{s=1}^m \mathcal{C}_s$, $\mathcal{C}_{s_1} \cap \mathcal{C}_{s_2} = \emptyset$, $s_1 \neq s_2$. For each node $i \in \mathcal{C}$, denote by $\hat{i}$ the cluster index satisfying $i \in \mathcal{C}_{\hat{i}}$. Without loss of generality, assume that each cluster consists of consecutive indices and can be expressed as

$$\mathcal{C}_s = \{\varpi_{s-1} + 1, \varpi_{s-1} + 2, \ldots, \varpi_s\}, \quad s = 1, 2, \ldots, m,$$

where $\varpi_0 = 0$, $\varpi_m = n$, and $1 \leq \varpi_{s-1} < \varpi_s \leq n$. Here, $\varpi_{s-1} + 1$ and ϖ_s represent the first and last nodes in cluster $\mathcal{C}_s$, respectively.

In what follows, we impose the following assumption.

$(CI)_1$ $a_i = a_j, b_i = b_j, \gamma_i = \gamma_j, \forall i, j \in c_s, s = 1, 2, \ldots, m.$

Assuming that Condition $(CI)_1$ holds, Systems (2.1), (2.2), and (2.3) can be reformulated in a compact vector representation as follows:

$$\begin{cases} \Delta^2 \mathbf{z}_{s,k}^{[\iota]} = 2(e^{-\frac{1}{2}\tilde{a}_s h} - 1)\Delta \mathbf{z}_{s,k}^{[\iota]} + \left[\dfrac{2 - 2e^{-\frac{1}{2}\tilde{a}_s h}}{\tilde{a}_s}\right]^2 \Big[\tilde{\gamma}_s \Delta_\iota^2 \mathbf{z}_{s,k}^{[\iota-1]} - \tilde{b}_s \mathbf{z}_{s,k}^{[\iota]} \\ \qquad + \displaystyle\sum_{s'=1}^m \tilde{c}_{ss'} F_{s'}(\mathbf{z}_{s',\delta_k}^{[\iota]}) + \frac{1}{\sqrt{h}} \sum_{s'=1}^m \tilde{\xi}_{ss'} \tilde{\varepsilon}_{s',k} \tilde{\sigma}_{s'}(\mathbf{z}_{s',o_k}^{[\iota]}) + \tilde{I}_s\Big], \quad \forall \iota \in (0, \aleph)_{\mathbb{Z}}, \\ \mathbf{z}_{s,\tau}^{[\iota]} = \tilde{\varphi}_{s,\tau}^{[\iota]}, \quad \forall \tau \in [-\delta_\infty, 1]_{\mathbb{Z}}, \iota \in (0, \aleph)_{\mathbb{Z}}, \\ \Delta_\iota \mathbf{z}_{s,k}^{[0]} = 0 = \Delta_\iota \mathbf{z}_{s,k}^{[\aleph-1]}, \end{cases} \tag{2.4}$$

where $k\in\mathbb{Z}_0, s=1,2,\ldots,m$; $\mathbf{z}_s=(z_{c_s^0},\ldots,z_{c_s^1})^T$, $\tilde{a}_s=a_{c_s^0}$, $\tilde{b}_s=b_{c_s^0}$, $\tilde{\gamma}_s=\gamma_{c_s^0}$, $\tilde{c}_{ss'}=[c_{ij}]_{c_s^0\le i\le c_s^1, c_{s'}^0\le j\le c_{s'}^1}$, $F_s(\mathbf{z}_s)=(f_{c_s^0}(z_{c_s^0}),\ldots,f_{c_s^1}(z_{c_s^1}))^T$, $\tilde{\xi}_{ss'}=[\xi_{ij}]_{c_s^0\le i\le c_s^1, c_{s'}^0\le j\le c_{s'}^1}$, $\tilde{\sigma}_s(\mathbf{z}_s)=(\sigma_{c_s^0}(z_{c_s^0}),\ldots,\sigma_{c_s^1}(z_{c_s^1}))^T$, $\tilde{\varepsilon}_s=\operatorname{diag}(\varepsilon_{c_s^0},\ldots,\varepsilon_{c_s^1})$, $\tilde{I}_s=(I_{c_s^0},\ldots,I_{c_s^1})^T$, $\tilde{\varphi}_s=(\varphi_{c_s^0},\ldots,\varphi_{c_s^1})^T$, $s,s'=1,2,\ldots,m$.

Following the same procedure, System (2.3) admits the clustering representation given below:

$$\begin{cases}\Delta^2\mathbf{w}_{s,k}^{[\iota]}=2(e^{-\frac{1}{2}\tilde{a}_sh}-1)\Delta\mathbf{w}_{s,k}^{[\iota]}+\left[\dfrac{2-2e^{-\frac{1}{2}\tilde{a}_sh}}{\tilde{a}_s}\right]^2\Big[\tilde{\gamma}_s\Delta_\iota^2\mathbf{w}_{s,k}^{[\iota-1]}-\tilde{b}_s\mathbf{w}_{s,k}^{[\iota]}\\ \qquad+\displaystyle\sum_{s'=1}^m\tilde{c}_{ss'}F_{s'}(\mathbf{w}_{s',\delta_k}^{[\iota]})+\frac{1}{\sqrt{h}}\sum_{s'=1}^m\tilde{\xi}_{ss'}\tilde{\varepsilon}_{s',k}\tilde{\sigma}_{s'}(\mathbf{w}_{s',o_k}^{[\iota]})+\tilde{I}_s\Big],\quad\forall\iota\in(0,\aleph)_{\mathbb{Z}},\\ \mathbf{w}_{s,\tau}^{[\iota]}=\tilde{\phi}_{s,\tau}^{[\iota]},\quad\forall\tau\in[-\delta_\infty,1]_{\mathbb{Z}},\iota\in(0,\aleph)_{\mathbb{Z}},\\ \Delta_\iota\mathbf{w}_{s,k}^{[0]}=0,\ \Delta_\iota\mathbf{w}_{s,k}^{[\aleph-1]}=\tilde{\rho}_{s,k},\end{cases}\tag{2.5}$$

where $k\in\mathbb{Z}_0$, $\mathbf{w}_s=(w_{c_s^0},\ldots,w_{c_s^1})^T$, $F_s(\mathbf{w}_s)=(f_{c_s^0}(w_{c_s^0}),\ldots,f_{c_s^1}(w_{c_s^1}))^T$, $\tilde{\sigma}_s(\mathbf{w}_s)=(\sigma_{c_s^0}(w_{c_s^0}),\ldots,\sigma_{c_s^1}(w_{c_s^1}))^T$, $\tilde{\phi}_s=(\phi_{c_s^0},\ldots,\phi_{c_s^1})^T$, $\tilde{\rho}_s=(\rho_{c_s^0},\ldots,\rho_{c_s^1})^T$, $s=1,2,\ldots,m$.

Define the synchronization error between Systems (2.4) and (2.5) as $\mathbf{e}_s=\mathbf{w}_s-\mathbf{z}_s$, for $s=1,2,\ldots,m$. Consequently,

$$\begin{cases}\Delta^2\mathbf{e}_{s,k}^{[\iota]}=2(e^{-\frac{1}{2}\tilde{a}_sh}-1)\Delta\mathbf{e}_{s,k}^{[\iota]}+\left[\dfrac{2-2e^{-\frac{1}{2}\tilde{a}_sh}}{\tilde{a}_s}\right]^2\\ \qquad\times\Big\{\tilde{\gamma}_s\Delta_\iota^2\mathbf{e}_{s,k}^{[\iota-1]}-\tilde{b}_s\mathbf{e}_{s,k}^{[\iota]}+\displaystyle\sum_{s'=1}^m\tilde{c}_{ss'}\Big[F_{s'}(\mathbf{w}_{s',\delta_k}^{[\iota]})-F_{s'}(\mathbf{z}_{s',\delta_k}^{[\iota]})\Big]\\ \qquad+\displaystyle\frac{1}{\sqrt{h}}\sum_{s'=1}^m\tilde{\xi}_{ss'}\tilde{\varepsilon}_{s',k}\Big[\tilde{\sigma}_{s'}(\mathbf{w}_{s',o_k}^{[\iota]})-\tilde{\sigma}_{s'}(\mathbf{z}_{s',o_k}^{[\iota]})\Big]\Big\},\quad\forall\iota\in(0,\aleph)_{\mathbb{Z}},\\ \mathbf{e}_{s,\tau}^{[\iota]}=\tilde{\varphi}_{s,\tau}^{[\iota]}-\tilde{\phi}_{s,\tau}^{[\iota]},\quad\forall\tau\in[-\delta_\infty,1]_{\mathbb{Z}},\iota\in(0,\aleph)_{\mathbb{Z}},\\ \Delta_\iota\mathbf{e}_{s,k}^{[0]}=0,\ \Delta_\iota\mathbf{e}_{s,k}^{[\aleph-1]}=\tilde{\rho}_{s,k},\end{cases}\tag{2.6}$$

where $k\in\mathbb{Z}_0$, $s=1,2,\ldots,m$.

An intermittent control strategy is imposed on the Reumann boundary and formulated as

$$\tilde{\rho}_{s,k}=\begin{cases}\alpha_s\displaystyle\sum_{\iota=1}^{\aleph-1}\mathbf{e}_{s,k}^{[\iota]}, & k\in[n\theta,n\theta+\beta)_{\mathbb{Z}},\\ 0, & k\in[n\theta+\beta,n\theta+\theta)_{\mathbb{Z}},\ n\in\mathbb{Z}_0,\end{cases}\tag{2.7}$$

where $\theta>\delta_\infty$ is a prescribed integer representing the control period, $\beta\in(0,\theta]_{\mathbb{Z}}$ denotes the active duration within each period, and α_s is the control gain associated with the sth cluster, $s=1,2,\ldots,m$.

Definition 2.1. *Under the intermittent BC* (2.7)*, the SINNs* (2.1) *are said to achieve m-cluster exponential synchronization (ES) in the mean-square sense if there exist constants* $\Xi>0$ *and* $\varkappa\in(0,1)$ *such that*

$$\sum_{s=1}^m\sum_{\iota=0}^{\aleph}\mathbb{E}\left\|\mathbf{w}_{s,k}^{[\iota]}-\mathbf{z}_{s,k}^{[\iota]}\right\|^2\le\Xi\varkappa^k,\quad\forall k\ge0.$$

Remark 2.1. *Taken together, [7–9] mainly investigated discrete-time and discrete-space SINNs from the perspectives of stability, periodicity, or antisynchronization. In particular, [8, 9] focused on single-network properties such as mean-square boundedness, exponential stability, and random periodic solutions, and [7] considered heterogeneous drive–response antisynchronization without involving clustered structures. In contrast, Model* (2.1) *in the present paper incorporates discrete time, discrete spatial diffusion, stochastic perturbations, inertial effects, and time delays within a clustered drive–response framework. This elevates the analysis from individual network dynamics to organized multigroup cooperative behavior, significantly enriching the structural complexity and coordination capacity of SINNs.*

3. Intermittent boundary synchronization

In this section, an intermittent boundary control scheme is proposed to realize mean-square exponential cluster synchronization for the considered clustered differencing SINNs. The control is applied periodically to boundary nodes, reducing control cost while maintaining synchronization performance. Based on a drive–response framework, the corresponding error system is derived with piecewise boundary actuation over control and rest intervals.

A discrete Lyapunov–Krasovskii functional is then constructed to account for inertia, diffusion, stochastic disturbances, and delays. By estimating its forward difference over both active and inactive periods, sufficient matrix inequality conditions are obtained to ensure mean-square exponential cluster synchronization, establishing the theoretical foundation of the proposed approach.

Let

$$\aleph_* = \frac{4}{\hbar^2}\cos^2\frac{\pi}{2\aleph-1}, \quad \mathscr{a}_s = 2(e^{-\frac{1}{2}\tilde{a}_s h}-1), \quad \mathscr{d}_s = \left[\frac{2-2e^{-\frac{1}{2}\tilde{a}_s h}}{\tilde{a}_s}\right]^2,$$

where $s = 1, 2, \ldots, m$. Then, the first equation of the error network (2.6) is turned into

$$\begin{aligned}\Delta^2\mathbf{e}^{[\iota]}_{s,k} \quad = \quad & \mathscr{a}_s\Delta\mathbf{e}^{[\iota]}_{s,k} + \mathscr{d}_s\tilde{\gamma}_s\Delta^2_\iota\mathbf{e}^{[\iota-1]}_{s,k} - \mathscr{d}_s\tilde{b}_s\mathbf{e}^{[\iota]}_{s,k} + \mathscr{d}_s\sum_{s'=1}^{m}\tilde{c}_{ss'}\Big[F_{s'}(\mathbf{w}^{[\iota]}_{s',\delta_k}) - F_{s'}(\mathbf{z}^{[\iota]}_{s',\delta_k})\Big] \\ & + \frac{1}{\sqrt{h}}\mathscr{d}_s\sum_{s'=1}^{m}\tilde{\xi}_{ss'}\tilde{\varepsilon}_{s',k}\Big[\tilde{\sigma}_{s'}(\mathbf{w}^{[\iota]}_{s',o_k}) - \tilde{\sigma}_{s'}(\mathbf{z}^{[\iota]}_{s',o_k})\Big], \quad \forall\iota\in(0,\aleph)_{\mathbb{Z}},\end{aligned} \tag{3.1}$$

where $k \in \mathbb{Z}_0$, $s = 1, 2, \ldots, m$.

To analyze System (3.1), a space–time discrete stochastic Lyapunov–Krasovskii functional (LKF) is proposed as

$$V_k = V_{1,k} + V_{2,k} + V_{3,k} + V_{4,k} + V_{5,k} + V_{6,k},$$

where

$$\begin{cases} V_{1,k} = \sum_{s=1}^{m}\sum_{\iota=1}^{\aleph-1}(\Delta\mathbf{e}_{s,k}^{[\iota]})^T P_s \Delta\mathbf{e}_{s,k}^{[\iota]}, \\ V_{2,k} = \lambda_P \sum_{s=1}^{m}\sum_{\iota=1}^{\aleph-1}(\mathbf{e}_{s,k}^{[\iota]})^T P_s \mathbf{e}_{s,k}^{[\iota]}, \\ V_{3,k} = \sum_{s=1}^{m}\sum_{\iota=1}^{\aleph-1}\sum_{l=1}^{\delta_\infty}\sum_{q=k-l}^{k-1}(\mathbf{e}_{s,q}^{[\iota]})^T \mathscr{L}_s^f W_s \mathscr{L}_s^f \mathbf{e}_{s,q}^{[\iota]}, \\ V_{4,k} = \frac{m}{h}\sum_{s=1}^{m}\sum_{\iota=1}^{\aleph-1}\sum_{l=1}^{\delta_\infty}\sum_{q=k-l}^{k-1}(\mathbf{e}_{s,q}^{[\iota]})^T Y_s \mathbf{e}_{s,q}^{[\iota]} \\ V_{5,k} = \sum_{s=1}^{m}\sum_{\iota=1}^{\aleph-1}\sum_{l=1}^{\delta_\infty}\sum_{q=k-l}^{k-1}\sum_{q'=q}^{k-1}(\mathbf{e}_{s,q'}^{[\iota]})^T \mathscr{L}_s^f W_s \mathscr{L}_s^f \mathbf{e}_{s,q'}^{[\iota]}, \\ V_{6,k} = \frac{m}{h}\sum_{s=1}^{m}\sum_{\iota=1}^{\aleph-1}\sum_{l=1}^{\delta_\infty}\sum_{q=k-l}^{k-1}\sum_{q'=q}^{k-1}(\mathbf{e}_{s,q'}^{[\iota]})^T Y_s \mathbf{e}_{s,q'}^{[\iota]}, \end{cases}$$

where $\lambda_P > 0$; $\mathscr{L}_s^f = \mathrm{diag}(L_{c_s^0}^f, L_{c_s^0+1}^f, \ldots, L_{c_s^1}^f)$; $\mathscr{L}_s^\sigma = \mathrm{diag}(L_{c_s^0}^\sigma, L_{c_s^0+1}^\sigma, \ldots, L_{c_s^1}^\sigma)$; and $W_s, Y_s > 0$ are diagonal, and $s = 1, 2, \ldots, m$. To facilitate the evaluation of the above LKF, the following assumptions are introduced.

$(CI)_2$ For any $u, v \in \mathbb{R}$,

$$|f_j(u) - f_j(v)| \leq L_j^f |u - v|, \quad |\sigma_j(u) - \sigma_j(v)| \leq L_j^\sigma |u - v|,$$

where $j = 1, 2, \ldots, n$.

$(CI)_3$ For each cluster $s = 1, 2, \ldots, m$, the following inequalities are valid:

$$(1 + 3\varepsilon^{-1} + \xi^{-1})m \sum_{s'=1}^{m} d_{s'}^2 \tilde{c}_{s's}^T P_{s'} \tilde{c}_{s's} \leq W_s, \quad \sum_{s'=1}^{m} d_{s'}^2 \mathscr{L}_s^\sigma \mathrm{ddiag}(\tilde{\xi}_{s's}^T P_{s'} \tilde{\xi}_{s's}) \mathscr{L}_s^\sigma \leq Y_s.$$

3.1. *Difference estimation of the Lyapunov–Krasovskii functional*

Based on the definition of LKF, we have

$$\begin{aligned} \mathbb{E}V_{1,k+1} &= \mathbb{E}\sum_{s=1}^{m}\sum_{\iota=1}^{\aleph-1}(\Delta\mathbf{e}_{s,k+1}^{[\iota]})^T P_s \Delta\mathbf{e}_{s,k+1}^{[\iota]} \\ &= \mathbb{E}\sum_{s=1}^{m}\sum_{\iota=1}^{\aleph-1}(\Delta\mathbf{e}_{s,k+1}^{[\iota]} - \Delta\mathbf{e}_{s,k}^{[\iota]} + \Delta\mathbf{e}_{s,k}^{[\iota]})^T P_s (\Delta\mathbf{e}_{s,k+1}^{[\iota]} - \Delta\mathbf{e}_{s,k}^{[\iota]} + \Delta\mathbf{e}_{s,k}^{[\iota]}) \\ &= \mathbb{E}\sum_{s=1}^{m}\sum_{\iota=1}^{\aleph-1}(\Delta^2\mathbf{e}_{s,k}^{[\iota]} + \Delta\mathbf{e}_{s,k}^{[\iota]})^T P_s (\Delta^2\mathbf{e}_{s,k}^{[\iota]} + \Delta\mathbf{e}_{s,k}^{[\iota]}) \\ &= \underbrace{\mathbb{E}\sum_{s=1}^{m}\sum_{\iota=1}^{\aleph-1}(\Delta^2\mathbf{e}_{s,k}^{[\iota]})^T P_s \Delta^2\mathbf{e}_{s,k}^{[\iota]}}_{\pounds_{1,k}} \end{aligned}$$

$$+\mathbb{E}\sum_{s=1}^{m}\sum_{\iota=1}^{\aleph-1}(\Delta\mathbf{e}_{s,k}^{[\iota]})^T P_s\Delta\mathbf{e}_{s,k}^{[\iota]}+\underbrace{2\mathbb{E}\sum_{s=1}^{m}\sum_{\iota=1}^{\aleph-1}(\Delta\mathbf{e}_{s,k}^{[\iota]})^T P_s\Delta^2\mathbf{e}_{s,k}^{[\iota]}}_{\pounds_{2,k}},\quad \forall k\in\mathbb{Z}_0. \tag{3.2}$$

In line with the error INN (3.1), it addresses

$$\begin{aligned}
\pounds_{1,k} &= \mathbb{E}\sum_{s=1}^{m}\sum_{\iota=1}^{\aleph-1}\Big\{a_s\Delta\mathbf{e}_{s,k}^{[\iota]}+d_s\Big[\tilde{\gamma}_s\Delta_\iota^2\mathbf{e}_{s,k}^{[\iota-1]}-\tilde{b}_s\mathbf{e}_{s,k}^{[\iota]}+\sum_{s'=1}^{m}\tilde{c}_{ss'}F_{s'}^*(\mathbf{e}_{s',\delta_k}^{[\iota]}) \\
&\quad+\frac{1}{\sqrt{h}}d_s\sum_{s'=1}^{m}\tilde{\xi}_{ss'}\tilde{\varepsilon}_{s',k}\tilde{\sigma}_{s'}^*(\mathbf{e}_{s',o_k}^{[\iota]})\Big]\Big\}^T P_s\Big\{a_s\Delta\mathbf{e}_{s,k}^{[\iota]}+d_s\Big[\tilde{\gamma}_s\Delta_\iota^2\mathbf{e}_{s,k}^{[\iota-1]} \\
&\quad-\tilde{b}_s\mathbf{e}_{s,k}^{[\iota]}+\sum_{s'=1}^{m}\tilde{c}_{ss'}F_{s'}^*(\mathbf{e}_{s',\delta_k}^{[\iota]})+\frac{1}{\sqrt{h}}d_s\sum_{s'=1}^{m}\tilde{\xi}_{ss'}\tilde{\varepsilon}_{s',k}\tilde{\sigma}_{s'}^*(\mathbf{e}_{s',o_k}^{[\iota]})\Big]\Big\} \\
&= \mathbb{E}\sum_{s=1}^{m}\sum_{\iota=1}^{\aleph-1}(\Delta\mathbf{e}_{s,k}^{[\iota]})^T a_s P_s a_s\Delta\mathbf{e}_{s,k}^{[\iota]}+\underbrace{2\mathbb{E}\sum_{s=1}^{m}\sum_{\iota=1}^{\aleph-1}(\Delta\mathbf{e}_{s,k}^{[\iota]})^T a_s P_s d_s\tilde{\gamma}_s\Delta_\iota^2\mathbf{e}_{s,k}^{[\iota-1]}}_{\mathsf{C}_{1,k}} \\
&\quad-2\mathbb{E}\sum_{s=1}^{m}\sum_{\iota=1}^{\aleph-1}(\Delta\mathbf{e}_{s,k}^{[\iota]})^T a_s P_s d_s\tilde{b}_s\mathbf{e}_{s,k}^{[\iota]}+\underbrace{2\mathbb{E}\sum_{s=1}^{m}\sum_{\iota=1}^{\aleph-1}(\Delta\mathbf{e}_{s,k}^{[\iota]})^T a_s P_s d_s\sum_{s'=1}^{m}\tilde{c}_{ss'}F_{s'}^*(\mathbf{e}_{s',\delta_k}^{[\iota]})}_{\mathsf{C}_{2,k}} \\
&\quad+\underbrace{\mathbb{E}\sum_{s=1}^{m}\sum_{\iota=1}^{\aleph-1}(\Delta_\iota^2\mathbf{e}_{s,k}^{[\iota-1]})^T\tilde{\gamma}_s d_s P_s d_s\tilde{\gamma}_s\Delta_\iota^2\mathbf{e}_{s,k}^{[\iota-1]}}_{\mathsf{C}_{3,k}}+\underbrace{(-2)\mathbb{E}\sum_{s=1}^{m}\sum_{\iota=1}^{\aleph-1}(\Delta_\iota^2\mathbf{e}_{s,k}^{[\iota-1]})^T\tilde{\gamma}_s d_s P_s d_s\tilde{b}_s\mathbf{e}_{s,k}^{[\iota]}}_{\mathsf{C}_{4,k}} \\
&\quad+\underbrace{2\mathbb{E}\sum_{s=1}^{m}\sum_{\iota=1}^{\aleph-1}(\Delta_\iota^2\mathbf{e}_{s,k}^{[\iota-1]})^T\tilde{\gamma}_s d_s P_s d_s\sum_{s'=1}^{m}\tilde{c}_{ss'}F_{s'}^*(\mathbf{e}_{s',\delta_k}^{[\iota]})}_{\mathsf{C}_{5,k}} \\
&\quad+\mathbb{E}\sum_{s=1}^{m}\sum_{\iota=1}^{\aleph-1}(\mathbf{e}_{s,k}^{[\iota]})^T\tilde{b}_s d_s P_s d_s\tilde{b}_s\mathbf{e}_{s,k}^{[\iota]} \\
&\quad+\underbrace{(-2)\mathbb{E}\sum_{s=1}^{m}\sum_{\iota=1}^{\aleph-1}(\mathbf{e}_{s,k}^{[\iota]})^T\tilde{b}_s d_s P_s d_s\sum_{s'=1}^{m}\tilde{c}_{ss'}F_{s'}^*(\mathbf{e}_{s',\delta_k}^{[\iota]})}_{\mathsf{C}_{6,k}} \\
&\quad+\underbrace{\mathbb{E}\sum_{s=1}^{m}\sum_{\iota=1}^{\aleph-1}\Big(\sum_{s'=1}^{m}\tilde{c}_{ss'}F_{s'}^*(\mathbf{e}_{s',\delta_k}^{[\iota]})\Big)^T d_s P_s d_s\sum_{s'=1}^{m}\tilde{c}_{ss'}F_{s'}^*(\mathbf{e}_{s',\delta_k}^{[\iota]})}_{\mathsf{C}_{7,k}} \\
&\quad+\underbrace{\frac{1}{h}\mathbb{E}\sum_{s=1}^{m}\sum_{\iota=1}^{\aleph-1}\Big(\sum_{s'=1}^{m}\tilde{\xi}_{ss'}\tilde{\varepsilon}_{s',k}\tilde{\sigma}_{s'}^*(\mathbf{e}_{s',o_k}^{[\iota]})\Big)^T d_s P_s d_s\sum_{s'=1}^{m}\tilde{\xi}_{ss'}\tilde{\varepsilon}_{s',k}\tilde{\sigma}_{s'}^*(\mathbf{e}_{s',o_k}^{[\iota]})}_{\mathsf{C}_{8,k}},
\end{aligned} \tag{3.3}$$

where $F^{*}_{s'}(\mathbf{e}^{[\iota]}_{s',\delta_k}) := F_{s'}(\mathbf{w}^{[\iota]}_{s',\delta_k}) - F_{s'}(\mathbf{z}^{[\iota]}_{s',\delta_k})$, $\tilde{\sigma}^{*}_{s'}(\mathbf{e}^{[\iota]}_{s',o_k}) := \tilde{\sigma}_{s'}(\mathbf{w}^{[\iota]}_{s',o_k}) - \tilde{\sigma}_{s'}(\mathbf{z}^{[\iota]}_{s',o_k})$, $k \in \mathbb{Z}_0$.

By using the Wirtinger-type inequality [7, Lemma 3.1], one has

$$\begin{aligned} \mathsf{C}_{1,k} &\leq \mathbb{E}\sum_{s=1}^{m}\sum_{\iota=1}^{\aleph-1} \mathscr{a}_s^2(\Delta\mathbf{e}^{[\iota]}_{s,k})^T P_s \Delta\mathbf{e}^{[\iota]}_{s,k} + \mathbb{E}\sum_{s=1}^{m}\sum_{\iota=1}^{\aleph-1} \mathscr{d}_s^2\tilde{\gamma}_s^2(\Delta_\iota^2\mathbf{e}^{[\iota-1]}_{s,k})^T P_s \Delta_\iota^2\mathbf{e}^{[\iota-1]}_{s,k} \qquad (3.4)\\ &\leq \varepsilon\mathbb{E}\sum_{s=1}^{m}\sum_{\iota=1}^{\aleph-1} \mathscr{a}_s^2(\Delta\mathbf{e}^{[\iota]}_{s,k})^T P_s \Delta\mathbf{e}^{[\iota]}_{s,k} + \frac{\aleph_*}{\varepsilon}\mathbb{E}\sum_{s=1}^{m}\sum_{\iota=1}^{\aleph-1} \mathscr{d}_s^2\tilde{\gamma}_s^2(\Delta_\iota\mathbf{e}^{[\iota]}_{s,k})^T P_s \Delta_\iota\mathbf{e}^{[\iota]}_{s,k}, \qquad (3.5) \end{aligned}$$

$$\begin{aligned} \mathsf{C}_{2,k} &\leq \varepsilon\mathbb{E}\sum_{s=1}^{m}\sum_{\iota=1}^{\aleph-1} \mathscr{a}_s^2(\Delta\mathbf{e}^{[\iota]}_{s,k})^T P_s \Delta\mathbf{e}^{[\iota]}_{s,k} + \frac{1}{\varepsilon}\mathbb{E}\sum_{s=1}^{m}\sum_{\iota=1}^{\aleph-1} \mathscr{d}_s^2\Big(\sum_{s'=1}^{m}\tilde{c}_{ss'}F^{*}_{s'}(\mathbf{e}^{[\iota]}_{s',\delta_k})\Big)^T P_s \sum_{s'=1}^{m}\tilde{c}_{ss'}F^{*}_{s'}(\mathbf{e}^{[\iota]}_{s',\delta_k})\\ &\leq \varepsilon\mathbb{E}\sum_{s=1}^{m}\sum_{\iota=1}^{\aleph-1} \mathscr{a}_s^2(\Delta\mathbf{e}^{[\iota]}_{s,k})^T P_s \Delta\mathbf{e}^{[\iota]}_{s,k} + \frac{1}{\varepsilon}m\mathbb{E}\sum_{s=1}^{m}\sum_{\iota=1}^{\aleph-1}\sum_{s'=1}^{m} \mathscr{d}_s^2\left[F^{*}_{s'}(\mathbf{e}^{[\iota]}_{s',\delta_k})\right]^T \tilde{c}^T_{ss'}P_s\tilde{c}_{ss'}F^{*}_{s'}(\mathbf{e}^{[\iota]}_{s',\delta_k})\\ &= \varepsilon\mathbb{E}\sum_{s=1}^{m}\sum_{\iota=1}^{\aleph-1} \mathscr{a}_s^2(\Delta\mathbf{e}^{[\iota]}_{s,k})^T P_s \Delta\mathbf{e}^{[\iota]}_{s,k} + \frac{m}{\varepsilon}\mathbb{E}\sum_{s=1}^{m}\sum_{\iota=1}^{\aleph-1}\left[F^{*}_{s}(\mathbf{e}^{[\iota]}_{s,\delta_k})\right]^T \Pi_s F^{*}_{s}(\mathbf{e}^{[\iota]}_{s,\delta_k}), \qquad (3.6) \end{aligned}$$

where $\Pi_s := \sum_{s'=1}^{m} \mathscr{d}_{s'}^2\tilde{c}^T_{s's}P_{s'}\tilde{c}_{s's}$,

$$\mathsf{C}_{3,k} \leq \aleph_*\mathbb{E}\sum_{s=1}^{m}\sum_{\iota=1}^{\aleph-1} \mathscr{d}_s^2\tilde{\gamma}_s^2(\Delta_\iota\mathbf{e}^{[\iota]}_{s,k})^T P_s \Delta_\iota\mathbf{e}^{[\iota]}_{s,k}, \qquad (3.7)$$

via the formula of the integral by parts [33]:

$$\begin{aligned} \mathsf{C}_{4,k} &= -2\mathbb{E}\sum_{s=1}^{m}\sum_{\iota=1}^{\aleph-1} \mathscr{d}_s^2\tilde{\gamma}_s\tilde{b}_s(\Delta_\iota^2\mathbf{e}^{[\iota-1]}_{s,k})^T P_s \mathbf{e}^{[\iota]}_{s,k}\\ &= -\frac{2}{\hbar}\mathbb{E}\sum_{s=1}^{m} \mathscr{d}_s^2\tilde{\gamma}_s\tilde{b}_s(\mathbf{e}^{[\aleph]}_{s,k})^T P_s\tilde{\rho}_{s,k} + 2\mathbb{E}\sum_{s=1}^{m}\sum_{\iota=1}^{\aleph-1} \mathscr{d}_s^2\tilde{\gamma}_s\tilde{b}_s(\Delta_\iota\mathbf{e}^{[\iota]}_{s,k})^T P_s\Delta_\iota\mathbf{e}^{[\iota]}_{s,k}, \qquad (3.8) \end{aligned}$$

$$\begin{aligned} \mathsf{C}_{5,k} &\leq \varepsilon\mathbb{E}\sum_{s=1}^{m}\sum_{\iota=1}^{\aleph-1} \mathscr{d}_s^2\tilde{\gamma}_s^2(\Delta_\iota^2\mathbf{e}^{[\iota-1]}_{s,k})^T P_s \Delta_\iota^2\mathbf{e}^{[\iota-1]}_{s,k}\\ &\quad + \frac{1}{\varepsilon}\mathbb{E}\sum_{s=1}^{m}\sum_{\iota=1}^{\aleph-1} \mathscr{d}_s^2\Big(\sum_{s'=1}^{m}\tilde{c}_{ss'}F^{*}_{s'}(\mathbf{e}^{[\iota]}_{s',\delta_k})\Big)^T P_s \sum_{s'=1}^{m}\tilde{c}_{ss'}F^{*}_{s'}(\mathbf{e}^{[\iota]}_{s',\delta_k})\\ &\leq \aleph_*\varepsilon\mathbb{E}\sum_{s=1}^{m}\sum_{\iota=1}^{\aleph-1} \mathscr{d}_s^2\tilde{\gamma}_s^2(\Delta_\iota\mathbf{e}^{[\iota]}_{s,k})^T P_s \Delta_\iota\mathbf{e}^{[\iota]}_{s,k}\\ &\quad + \frac{m}{\varepsilon}\mathbb{E}\sum_{s=1}^{m}\sum_{\iota=1}^{\aleph-1}\sum_{s'=1}^{m} \mathscr{d}_s^2\left[F^{*}_{s'}(\mathbf{e}^{[\iota]}_{s',\delta_k})\right]^T \tilde{c}^T_{ss'}P_s\tilde{c}_{ss'}F^{*}_{s'}(\mathbf{e}^{[\iota]}_{s',\delta_k})\\ &= \aleph_*\varepsilon\mathbb{E}\sum_{s=1}^{m}\sum_{\iota=1}^{\aleph-1} \mathscr{d}_s^2\tilde{\gamma}_s^2(\Delta_\iota\mathbf{e}^{[\iota]}_{s,k})^T P_s \Delta_\iota\mathbf{e}^{[\iota]}_{s,k} \end{aligned}$$

$$+\frac{m}{\varepsilon}\mathbb{E}\sum_{s=1}^{m}\sum_{\iota=1}^{\aleph-1}\left[F_s^*(\mathbf{e}_{s,\delta_k}^{[\iota]})\right]^T\Pi_s F_s^*(\mathbf{e}_{s,\delta_k}^{[\iota]}), \tag{3.9}$$

$$\mathsf{C}_{6,k}\leq\varepsilon\mathbb{E}\sum_{s=1}^{m}\sum_{\iota=1}^{\aleph-1}d_s^2\tilde{b}_s^2(\mathbf{e}_{s,k}^{[\iota]})^T P_s\mathbf{e}_{s,k}^{[\iota]}+\frac{m}{\varepsilon}\mathbb{E}\sum_{s=1}^{m}\sum_{\iota=1}^{\aleph-1}\left[F_s^*(\mathbf{e}_{s,\delta_k}^{[\iota]})\right]^T\Pi_s F_s^*(\mathbf{e}_{s,\delta_k}^{[\iota]}), \tag{3.10}$$

$$\mathsf{C}_{7,k}\leq m\mathbb{E}\sum_{s=1}^{m}\sum_{\iota=1}^{\aleph-1}\left[F_s^*(\mathbf{e}_{s,\delta_k}^{[\iota]})\right]^T\Pi_s F_s^*(\mathbf{e}_{s,\delta_k}^{[\iota]}). \tag{3.11}$$

Furthermore, by Assumption $(CI)_2$, aligned

$$\begin{aligned}
\mathsf{C}_{8,k} &\leq \frac{m}{h}\mathbb{E}\sum_{s=1}^{m}\sum_{\iota=1}^{\aleph-1}\sum_{s'=1}^{m}d_s^2\left[\tilde{\sigma}_{s'}^*(\mathbf{e}_{s',o_k}^{[\iota]})\right]^T\mathrm{ddiag}(\tilde{\xi}_{ss'}^T P_s\tilde{\xi}_{ss'})\tilde{\sigma}_{s'}^*(\mathbf{e}_{s',o_k}^{[\iota]})\\
&\leq \frac{m}{h}\mathbb{E}\sum_{s=1}^{m}\sum_{\iota=1}^{\aleph-1}\sum_{s'=1}^{m}d_s^2(\mathbf{e}_{s',o_k}^{[\iota]})^T\mathscr{L}_{s'}^{\sigma}\mathrm{ddiag}(\tilde{\xi}_{ss'}^T P_s\tilde{\xi}_{ss'})\mathscr{L}_{s'}^{\sigma}\mathbf{e}_{s',o_k}^{[\iota]}\\
&= \frac{m}{h}\mathbb{E}\sum_{s=1}^{m}\sum_{\iota=1}^{\aleph-1}(\mathbf{e}_{s,o_k}^{[\iota]})^T Y_s\mathbf{e}_{s,o_k}^{[\iota]},\quad\forall k\in\mathbb{Z}_0.
\end{aligned} \tag{3.12}$$

Substituting (3.4)–(3.12) into (3.3) leads to the following.

Proposition 3.1. *For any $k\in\mathbb{Z}_0$, we have*

$$\begin{aligned}
\pounds_{1,k} &\leq (1+\varepsilon)\mathbb{E}\sum_{s=1}^{m}\sum_{\iota=1}^{\aleph-1}d_s^2\tilde{b}_s^2(\mathbf{e}_{s,k}^{[\iota]})^T P_s\mathbf{e}_{s,k}^{[\iota]}-2\mathbb{E}\sum_{s=1}^{m}\sum_{\iota=1}^{\aleph-1}a_s d_s\tilde{b}_s(\Delta\mathbf{e}_{s,k}^{[\iota]})^T P_s\mathbf{e}_{s,k}^{[\iota]}\\
&\quad+(1+2\varepsilon)\mathbb{E}\sum_{s=1}^{m}\sum_{\iota=1}^{\aleph-1}a_s^2(\Delta\mathbf{e}_{s,k}^{[\iota]})^T P_s\Delta\mathbf{e}_{s,k}^{[\iota]}-\frac{2}{\hbar}\mathbb{E}\sum_{s=1}^{m}\sum_{\iota=1}^{\aleph-1}d_s^2\tilde{\gamma}_s\tilde{b}_s(\mathbf{e}_{s,k}^{[\aleph]})^T P_s\tilde{\rho}_{s,k}\\
&\quad+\mathbb{E}\sum_{s=1}^{m}\sum_{\iota=1}^{\aleph-1}d_s^2((1+\varepsilon+\varepsilon^{-1})\aleph_*\tilde{\gamma}_s^2+2\tilde{\gamma}_s\tilde{b}_s)(\Delta_\iota\mathbf{e}_{s,k}^{[\iota]})^T P_s\Delta_\iota\mathbf{e}_{s,k}^{[\iota]}\\
&\quad+(1+3\varepsilon^{-1})m\mathbb{E}\sum_{s=1}^{m}\sum_{\iota=1}^{\aleph-1}\left[F_s^*(\mathbf{e}_{s,\delta_k}^{[\iota]})\right]^T\Pi_s F_s^*(\mathbf{e}_{s,\delta_k}^{[\iota]})+\frac{m}{h}\mathbb{E}\sum_{s=1}^{m}\sum_{\iota=1}^{\aleph-1}(\mathbf{e}_{s,o_k}^{[\iota]})^T Y_s\mathbf{e}_{s,o_k}^{[\iota]}.
\end{aligned} \tag{3.13}$$

Additionally,

$$\begin{aligned}
\pounds_{2,k} &= 2\mathbb{E}\sum_{s=1}^{m}\sum_{\iota=1}^{\aleph-1}(\Delta\mathbf{e}_{s,k}^{[\iota]})^T P_s\Bigg\{a_s\Delta\mathbf{e}_{s,k}^{[\iota]}+d_s\Bigg[\tilde{\gamma}_s\Delta_\iota^2\mathbf{e}_{s,k}^{[\iota-1]}-\tilde{b}_s\mathbf{e}_{s,k}^{[\iota]}\\
&\quad+\sum_{s'=1}^{m}\tilde{c}_{ss'}F_{s'}^*(\mathbf{e}_{s',\delta_k}^{[\iota]})+\frac{1}{\sqrt{h}}d_s\sum_{s'=1}^{m}\tilde{\xi}_{ss'}\tilde{\varepsilon}_{s',k}\tilde{\sigma}_{s'}^*(\mathbf{e}_{s',o_k}^{[\iota]})\Bigg]\Bigg\}
\end{aligned}$$

$$= 2\mathbb{E}\sum_{s=1}^{m}\sum_{\iota=1}^{\aleph-1}(\Delta\mathbf{e}_{s,k}^{[\iota]})^T P_s \mathscr{a}_s \Delta\mathbf{e}_{s,k}^{[\iota]} + \underbrace{2\mathbb{E}\sum_{s=1}^{m}\sum_{\iota=1}^{\aleph-1}(\Delta\mathbf{e}_{s,k}^{[\iota]})^T P_s \mathscr{d}_s \tilde{\gamma}_s \Delta_\iota^2 \mathbf{e}_{s,k}^{[\iota-1]}}_{\mathscr{B}_{1,k}}$$

$$-2\mathbb{E}\sum_{s=1}^{m}\sum_{\iota=1}^{\aleph-1}(\Delta\mathbf{e}_{s,k}^{[\iota]})^T P_s \mathscr{d}_s \tilde{b}_s \mathbf{e}_{s,k}^{[\iota]} + \underbrace{2\mathbb{E}\sum_{s=1}^{m}\sum_{\iota=1}^{\aleph-1}(\Delta\mathbf{e}_{s,k}^{[\iota]})^T P_s \mathscr{d}_s \sum_{s'=1}^{m}\tilde{c}_{ss'}F_{s'}^*(\mathbf{e}_{s',\delta_k}^{[\iota]})}_{\mathscr{B}_{2,k}}, \quad (3.14)$$

in which

$$\begin{aligned}
\mathscr{B}_{1,k} &\le \xi\mathbb{E}\sum_{s=1}^{m}\sum_{\iota=1}^{\aleph-1}(\Delta\mathbf{e}_{s,k}^{[\iota]})^T P_s \Delta\mathbf{e}_{s,k}^{[\iota]} + \frac{1}{\xi}\mathbb{E}\sum_{s=1}^{m}\sum_{\iota=1}^{\aleph-1}\mathscr{d}_s^2\tilde{\gamma}_s^2(\Delta_\iota^2\mathbf{e}_{s,k}^{[\iota-1]})^T P_s \Delta_\iota^2 \mathbf{e}_{s,k}^{[\iota-1]} \\
&\le \xi\mathbb{E}\sum_{s=1}^{m}\sum_{\iota=1}^{\aleph-1}(\Delta\mathbf{e}_{s,k}^{[\iota]})^T P_s \Delta\mathbf{e}_{s,k}^{[\iota]} + \frac{\aleph_*}{\xi}\mathbb{E}\sum_{s=1}^{m}\sum_{\iota=1}^{\aleph-1}\mathscr{d}_s^2\tilde{\gamma}_s^2(\Delta_\iota\mathbf{e}_{s,k}^{[\iota]})^T P_s \Delta_\iota \mathbf{e}_{s,k}^{[\iota]}, \quad (3.15)
\end{aligned}$$

$$\begin{aligned}
\mathscr{B}_{2,k} &\le \xi\mathbb{E}\sum_{s=1}^{m}\sum_{\iota=1}^{\aleph-1}(\Delta\mathbf{e}_{s,k}^{[\iota]})^T P_s \Delta\mathbf{e}_{s,k}^{[\iota]} + \frac{1}{\xi}\mathbb{E}\sum_{s=1}^{m}\sum_{\iota=1}^{\aleph-1}\mathscr{d}_s^2\Big(\sum_{s'=1}^{m}\tilde{c}_{ss'}F_{s'}^*(\mathbf{e}_{s',\delta_k}^{[\iota]})\Big)^T P_s \sum_{s'=1}^{m}\tilde{c}_{ss'}F_{s'}^*(\mathbf{e}_{s',\delta_k}^{[\iota]}) \\
&\le \xi\mathbb{E}\sum_{s=1}^{m}\sum_{\iota=1}^{\aleph-1}(\Delta\mathbf{e}_{s,k}^{[\iota]})^T P_s \Delta\mathbf{e}_{s,k}^{[\iota]} + \frac{m}{\xi}\mathbb{E}\sum_{s=1}^{m}\sum_{\iota=1}^{\aleph-1}\sum_{s'=1}^{m}\mathscr{d}_s^2\left[F_{s'}^*(\mathbf{e}_{s',\delta_k}^{[\iota]})\right]^T \tilde{c}_{ss'}^T P_s \tilde{c}_{ss'}F_{s'}^*(\mathbf{e}_{s',\delta_k}^{[\iota]}) \\
&= \xi\mathbb{E}\sum_{s=1}^{m}\sum_{\iota=1}^{\aleph-1}(\Delta\mathbf{e}_{s,k}^{[\iota]})^T P_s \Delta\mathbf{e}_{s,k}^{[\iota]} + \frac{m}{\xi}\mathbb{E}\sum_{s=1}^{m}\sum_{\iota=1}^{\aleph-1}\left[F_s^*(\mathbf{e}_{s,\delta_k}^{[\iota]})\right]^T \Pi_s F_s^*(\mathbf{e}_{s,\delta_k}^{[\iota]}), \quad (3.16)
\end{aligned}$$

where $k \in \mathbb{Z}_0$.

In line with (3.14)–(3.16), we attain

Proposition 3.2. *For any $k \in \mathbb{Z}_0$, we have*

$$\begin{aligned}
\pounds_{2,k} &\le -2\mathbb{E}\sum_{s=1}^{m}\sum_{\iota=1}^{\aleph-1}\mathscr{d}_s\tilde{b}_s(\Delta\mathbf{e}_{s,k}^{[\iota]})^T P_s \mathbf{e}_{s,k}^{[\iota]} + \mathbb{E}\sum_{s=1}^{m}\sum_{\iota=1}^{\aleph-1}2(\mathscr{a}_s+\xi)(\Delta\mathbf{e}_{s,k}^{[\iota]})^T P_s \Delta\mathbf{e}_{s,k}^{[\iota]} \\
&\quad + \frac{\aleph_*}{\xi}\mathbb{E}\sum_{s=1}^{m}\sum_{\iota=1}^{\aleph-1}\mathscr{d}_s^2\tilde{\gamma}_s^2(\Delta_\iota\mathbf{e}_{s,k}^{[\iota]})^T P_s \Delta_\iota \mathbf{e}_{s,k}^{[\iota]} + \frac{m}{\xi}\mathbb{E}\sum_{s=1}^{m}\sum_{\iota=1}^{\aleph-1}\left[F_s^*(\mathbf{e}_{s,\delta_k}^{[\iota]})\right]^T \Pi_s F_s^*(\mathbf{e}_{s,\delta_k}^{[\iota]}). \quad (3.17)
\end{aligned}$$

Replacing $\pounds_1$ and $\pounds_2$ in (3.2) by the right sides of (3.13) and (3.17) respectively, we get the following.

Proposition 3.3. *For any $k \in \mathbb{Z}_0$, we have*

$$\begin{aligned}
\mathbb{E}(\Delta V_{1,k}) &\le (1+\varepsilon)\mathbb{E}\sum_{s=1}^{m}\sum_{\iota=1}^{\aleph-1}\mathscr{d}_s^2\tilde{b}_s^2(\mathbf{e}_{s,k}^{[\iota]})^T P_s \mathbf{e}_{s,k}^{[\iota]} - 2\mathbb{E}\sum_{s=1}^{m}\sum_{\iota=1}^{\aleph-1}(1+\mathscr{a}_s)\mathscr{d}_s\tilde{b}_s(\Delta\mathbf{e}_{s,k}^{[\iota]})^T P_s \mathbf{e}_{s,k}^{[\iota]} \\
&\quad + \mathbb{E}\sum_{s=1}^{m}\sum_{\iota=1}^{\aleph-1}[(1+2\varepsilon)\mathscr{a}_s^2 + 2\mathscr{a}_s + 2\xi](\Delta\mathbf{e}_{s,k}^{[\iota]})^T P_s \Delta\mathbf{e}_{s,k}^{[\iota]}
\end{aligned}$$

$$
\begin{aligned}
&+\mathbb{E}\sum_{s=1}^{m}\sum_{\iota=1}^{\aleph-1} d_s^2((1+\varepsilon+\varepsilon^{-1}+\xi^{-1})\aleph_*\tilde{\gamma}_s^2+2\tilde{\gamma}_s\tilde{b}_s)(\Delta_\iota \mathbf{e}_{s,k}^{[\iota]})^T P_s \Delta_\iota \mathbf{e}_{s,k}^{[\iota]} \\
&+(1+3\varepsilon^{-1}+\xi^{-1})m\mathbb{E}\sum_{s=1}^{m}\sum_{\iota=1}^{\aleph-1}\left[F_s^*(\mathbf{e}_{s,\delta_k}^{[\iota]})\right]^T \Pi_s F_s^*(\mathbf{e}_{s,\delta_k}^{[\iota]}) + \frac{m}{h}\mathbb{E}\sum_{s=1}^{m}\sum_{\iota=1}^{\aleph-1}(\mathbf{e}_{s,o_k}^{[\iota]})^T Y_s \mathbf{e}_{s,o_k}^{[\iota]} \\
&\underbrace{-\frac{2}{\hbar}\mathbb{E}\sum_{s=1}^{m} d_s^2\tilde{\gamma}_s\tilde{b}_s(\mathbf{e}_{s,k}^{[\aleph]})^T P_s\tilde{\rho}_{s,k}}_{\S_{1,k}}, \quad \forall k\in\mathbb{Z}_0.
\end{aligned} \tag{3.18}
$$

In line with Model (3.1), we attain

$$
\begin{aligned}
\mathbb{E}(\Delta V_{2,k}) &= \lambda_P\mathbb{E}\sum_{s=1}^{m}\sum_{\iota=1}^{\aleph-1}(\mathbf{e}_{s,k+1}^{[\iota]})^T P_s \mathbf{e}_{s,k+1}^{[\iota]} - \mathbb{E}V_{2,k} \\
&= \lambda_P\mathbb{E}\sum_{s=1}^{m}\sum_{\iota=1}^{\aleph-1}(\mathbf{e}_{s,k+1}^{[\iota]}-\mathbf{e}_{s,k}^{[\iota]}+\mathbf{e}_{s,k}^{[\iota]})^T P_s(\mathbf{e}_{s,k+1}^{[\iota]}-\mathbf{e}_{s,k}^{[\iota]}+\mathbf{e}_{s,k}^{[\iota]}) - \mathbb{E}V_{2,k} \\
&= \lambda_P\mathbb{E}\sum_{s=1}^{m}\sum_{\iota=1}^{\aleph-1}(\Delta\mathbf{e}_{s,k}^{[\iota]})^T P_s\Delta\mathbf{e}_{s,k}^{[\iota]} + 2\lambda_P\mathbb{E}\sum_{s=1}^{m}\sum_{\iota=1}^{\aleph-1}(\mathbf{e}_{s,k}^{[\iota]})^T P_s\Delta\mathbf{e}_{s,k}^{[\iota]}, \quad \forall k\in\mathbb{Z}_0.
\end{aligned} \tag{3.19}
$$

3.2. Treatment of nonlinearities and time delays

On account of the condition $(CI)_2$, we take

$$
\begin{aligned}
0 &= \mathbb{E}\sum_{s=1}^{m}\sum_{\iota=1}^{\aleph-1}\left[F_s^*(\mathbf{e}_{s,\delta_k}^{[\iota]})\right]^T W_s F_s^*(\mathbf{e}_{s,\delta_k}^{[\iota]}) - \mathbb{E}\sum_{s=1}^{m}\sum_{\iota=1}^{\aleph-1}\left[F_s^*(\mathbf{e}_{s,\delta_k}^{[\iota]})\right]^T W_s F_s^*(\mathbf{e}_{s,\delta_k}^{[\iota]}) \\
&\leq \mathbb{E}\sum_{s=1}^{m}\sum_{\iota=1}^{\aleph-1}(\mathbf{e}_{s,\delta_k}^{[\iota]})^T \mathscr{L}_s^f W_s \mathscr{L}_s^f \mathbf{e}_{s,\delta_k}^{[\iota]} - \mathbb{E}\sum_{s=1}^{m}\sum_{\iota=1}^{\aleph-1}\left[F_s^*(\mathbf{e}_{s,\delta_k}^{[\iota]})\right]^T W_s F_s^*(\mathbf{e}_{s,\delta_k}^{[\iota]}), \quad \forall k\in\mathbb{Z}_0.
\end{aligned} \tag{3.20}
$$

In accordance with the preceding definition of V_3, we can infer that

$$
\begin{aligned}
\mathbb{E}(\Delta V_{3,k}) &= \mathbb{E}V_{3,k+1} - \mathbb{E}V_{3,k} \\
&= \mathbb{E}\sum_{s=1}^{m}\sum_{\iota=1}^{\aleph-1}\sum_{l=1}^{\delta_\infty}\sum_{q=k+1-l}^{k}(\mathbf{e}_{s,q}^{[\iota]})^T \mathscr{L}_s^f W_s \mathscr{L}_s^f \mathbf{e}_{s,q}^{[\iota]} \\
&\quad -\mathbb{E}\sum_{s=1}^{m}\sum_{\iota=1}^{\aleph-1}\sum_{l=1}^{\delta_\infty}\sum_{q=k-l}^{k-1}(\mathbf{e}_{s,q}^{[\iota]})^T \mathscr{L}_s^f W_s \mathscr{L}_s^f \mathbf{e}_{s,q}^{[\iota]} \\
&= \mathbb{E}\sum_{s=1}^{m}\sum_{\iota=1}^{\aleph-1}\sum_{l=1}^{\delta_\infty}(\mathbf{e}_{s,k}^{[\iota]})^T \mathscr{L}_s^f W_s \mathscr{L}_s^f \mathbf{e}_{s,k}^{[\iota]} \\
&\quad +\mathbb{E}\sum_{s=1}^{m}\sum_{\iota=1}^{\aleph-1}\sum_{l=1}^{\delta_\infty}\sum_{q=k+1-l}^{k-1}(\mathbf{e}_{s,q}^{[\iota]})^T \mathscr{L}_s^f W_s \mathscr{L}_s^f \mathbf{e}_{s,q}^{[\iota]}
\end{aligned}
$$

$$
\begin{aligned}
& -\mathbb{E}\sum_{s=1}^{m}\sum_{\iota=1}^{\aleph-1}\sum_{l=1}^{\delta_\infty}\sum_{q=k-l}^{k-1}(\mathbf{e}_{s,q}^{[\iota]})^T\mathscr{L}_s^f W_s\mathscr{L}_s^f\mathbf{e}_{s,q}^{[\iota]} \\
= \;& \delta_\infty\mathbb{E}\sum_{s=1}^{m}\sum_{\iota=1}^{\aleph-1}(\mathbf{e}_{s,k}^{[\iota]})^T\mathscr{L}_s^f W_s\mathscr{L}_s^f\mathbf{e}_{s,k}^{[\iota]} - \mathbb{E}\sum_{s=1}^{m}\sum_{\iota=1}^{\aleph-1}\sum_{l=1}^{\delta_\infty}(\mathbf{e}_{s,k-l}^{[\iota]})^T\mathscr{L}_s^f W_s\mathscr{L}_s^f\mathbf{e}_{s,k-l}^{[\iota]} \\
\leq \;& \delta_\infty\mathbb{E}\sum_{s=1}^{m}\sum_{\iota=1}^{\aleph-1}(\mathbf{e}_{s,k}^{[\iota]})^T\mathscr{L}_s^f W_s\mathscr{L}_s^f\mathbf{e}_{s,k}^{[\iota]} - \mathbb{E}\sum_{s=1}^{m}\sum_{\iota=1}^{\aleph-1}(\mathbf{e}_{s,\delta_k}^{[\iota]})^T\mathscr{L}_s^f W_s\mathscr{L}_s^f\mathbf{e}_{s,\delta_k}^{[\iota]}; \qquad (3.21)
\end{aligned}
$$

likewise,

$$
\begin{aligned}
\mathbb{E}(\Delta V_{4,k}) = \;& \mathbb{E}V_{4,k+1} - \mathbb{E}V_{4,k} \\
= \;& \frac{m}{h}\mathbb{E}\sum_{s=1}^{m}\sum_{\iota=1}^{\aleph-1}\sum_{l=1}^{\delta_\infty}\left[\sum_{q=k+1-l}^{k}(\mathbf{e}_{s,q}^{[\iota]})^T Y_s\mathbf{e}_{s,q}^{[\iota]} - \sum_{q=k-l}^{k-1}(\mathbf{e}_{s,q}^{[\iota]})^T Y_s\mathbf{e}_{s,q}^{[\iota]}\right] \\
= \;& \frac{m}{h}\mathbb{E}\sum_{s=1}^{m}\sum_{\iota=1}^{\aleph-1}\sum_{l=1}^{\delta_\infty}\left[(\mathbf{e}_{s,k}^{[\iota]})^T Y_s\mathbf{e}_{s,k}^{[\iota]} - (\mathbf{e}_{s,k-l}^{[\iota]})^T Y_s\mathbf{e}_{s,k-l}^{[\iota]}\right] \\
= \;& \frac{m\delta_\infty}{h}\mathbb{E}\sum_{s=1}^{m}\sum_{\iota=1}^{\aleph-1}(\mathbf{e}_{s,k}^{[\iota]})^T Y_s\mathbf{e}_{s,k}^{[\iota]} - \frac{m}{h}\mathbb{E}\sum_{s=1}^{m}\sum_{\iota=1}^{\aleph-1}\sum_{l=1}^{\delta_\infty}(\mathbf{e}_{s,k-l}^{[\iota]})^T Y_s\mathbf{e}_{s,k-l}^{[\iota]} \\
\leq \;& \frac{m\delta_\infty}{h}\mathbb{E}\sum_{s=1}^{m}\sum_{\iota=1}^{\aleph-1}(\mathbf{e}_{s,k}^{[\iota]})^T Y_s\mathbf{e}_{s,k}^{[\iota]} - \frac{m}{h}\mathbb{E}\sum_{s=1}^{m}\sum_{\iota=1}^{\aleph-1}(\mathbf{e}_{s,o_k}^{[\iota]})^T Y_s\mathbf{e}_{s,o_k}^{[\iota]}, \quad \forall k\in\mathbb{Z}_0. \qquad (3.22)
\end{aligned}
$$

Additionally,

$$
\begin{aligned}
\mathbb{E}(\Delta V_{5,k}) = \;& \sum_{s=1}^{m}\sum_{\iota=1}^{\aleph-1}\sum_{l=1}^{\delta_\infty}\sum_{q=k+1-l}^{k}\sum_{q'=q}^{k}(\mathbf{e}_{s,q'}^{[\iota]})^T\mathscr{L}_s^f W_s\mathscr{L}_s^f\mathbf{e}_{s,q'}^{[\iota]} - V_{5,k} \\
= \;& \sum_{s=1}^{m}\sum_{\iota=1}^{\aleph-1}\sum_{l=1}^{\delta_\infty}(\mathbf{e}_{s,k}^{[\iota]})^T\mathscr{L}_s^f W_s\mathscr{L}_s^f\mathbf{e}_{s,k}^{[\iota]} + \sum_{s=1}^{m}\sum_{\iota=1}^{\aleph-1}\sum_{l=1}^{\delta_\infty}\sum_{q=k+1-l}^{k-1}(\mathbf{e}_{s,k}^{[\iota]})^T\mathscr{L}_s^f W_s\mathscr{L}_s^f\mathbf{e}_{s,k}^{[\iota]} \\
& + \sum_{s=1}^{m}\sum_{\iota=1}^{\aleph-1}\sum_{l=1}^{\delta_\infty}\sum_{q=k+1-l}^{k-1}\sum_{q'=q}^{k-1}(\mathbf{e}_{s,q'}^{[\iota]})^T\mathscr{L}_s^f W_s\mathscr{L}_s^f\mathbf{e}_{s,q'}^{[\iota]} \\
& - \sum_{s=1}^{m}\sum_{\iota=1}^{\aleph-1}\sum_{l=1}^{\delta_\infty}\sum_{q=k-l}^{k-1}\sum_{q'=q}^{k-1}(\mathbf{e}_{s,q'}^{[\iota]})^T\mathscr{L}_s^f W_s\mathscr{L}_s^f\mathbf{e}_{s,q'}^{[\iota]} \\
\leq \;& \delta_\infty\sum_{s=1}^{m}\sum_{\iota=1}^{\aleph-1}(\mathbf{e}_{s,k}^{[\iota]})^T\mathscr{L}_s^f W_s\mathscr{L}_s^f\mathbf{e}_{s,k}^{[\iota]} + \delta_\infty^2\sum_{s=1}^{m}\sum_{\iota=1}^{\aleph-1}(\mathbf{e}_{s,k}^{[\iota]})^T\mathscr{L}_s^f W_s\mathscr{L}_s^f\mathbf{e}_{s,k}^{[\iota]} \\
& - \sum_{s=1}^{m}\sum_{\iota=1}^{\aleph-1}\sum_{l=1}^{\delta_\infty}\sum_{q'=k-l}^{k-1}(\mathbf{e}_{s,q'}^{[\iota]})^T\mathscr{L}_s^f W_s\mathscr{L}_s^f\mathbf{e}_{s,q'}^{[\iota]} \\
= \;& \delta_\infty(\delta_\infty+1)\sum_{s=1}^{m}\sum_{\iota=1}^{\aleph-1}(\mathbf{e}_{s,k}^{[\iota]})^T\mathscr{L}_s^f W_s\mathscr{L}_s^f\mathbf{e}_{s,k}^{[\iota]} - V_{3,k}, \qquad (3.23)
\end{aligned}
$$

and likewise,

$$\mathbb{E}(\Delta V_{6,k}) \leq \delta_\infty(\delta_\infty + 1)\frac{m}{h}\sum_{s=1}^{m}\sum_{\iota=1}^{\aleph-1}(\mathbf{e}_{s,k}^{[\iota]})^T Y_s \mathbf{e}_{s,k}^{[\iota]} - V_{4,k}, \tag{3.24}$$

$$\begin{aligned} \mathbb{E}(V_{5,k}) &\leq \sum_{s=1}^{m}\sum_{\iota=1}^{\aleph-1}\sum_{l=1}^{\delta_\infty}\sum_{q=k-l}^{k-1}\sum_{q'=k-l}^{k-1}(\mathbf{e}_{s,q'}^{[\iota]})^T \mathscr{L}_s^f W_s \mathscr{L}_s^f \mathbf{e}_{s,q'}^{[\iota]} \\ &\leq \delta_\infty \sum_{s=1}^{m}\sum_{\iota=1}^{\aleph-1}\sum_{l=1}^{\delta_\infty}\sum_{q=k-l}^{k-1}(\mathbf{e}_{s,q}^{[\iota]})^T \mathscr{L}_s^f W_s \mathscr{L}_s^f \mathbf{e}_{s,q}^{[\iota]} = \delta_\infty V_{3,k}, \end{aligned} \tag{3.25}$$

and $\mathbb{E}(V_{6,k}) \leq \delta_\infty V_{4,k}$, $k \in \mathbb{Z}_0$.

3.3. Design of intermittent boundary control

By (3.18) and (2.7), $\S_{1,k} = 0$ for $k \in [n\theta + \beta, n\theta + \theta)_{\mathbb{Z}}$, and when $k \in [n\theta, n\theta + \beta)_{\mathbb{Z}}$, we have

$$\S_{1,k} = \frac{2}{\hbar}\mathbb{E}\sum_{s=1}^{m}\sum_{\iota=1}^{\aleph-1} d_s^2 \tilde{\gamma}_s \tilde{b}_s (\mathbf{e}_{s,k}^{[\aleph]})^T P_s \alpha_s \mathbf{e}_{s,k}^{[\iota]},$$

which implies that by letting $\vec{\mathbf{e}}_{s,k}^{[\iota]} = \mathbf{e}_{s,k}^{[\aleph]} - \mathbf{e}_{s,k}^{[\iota]}$,

$$\S_{1,k} = \frac{2}{\hbar}\mathbb{E}\sum_{s=1}^{m}\sum_{\iota=1}^{\aleph-1} d_s^2 \tilde{\gamma}_s \tilde{b}_s \Big[(\vec{\mathbf{e}}_{s,k}^{[\iota]})^T P_s \alpha_s \mathbf{e}_{s,k}^{[\iota]} + (\mathbf{e}_{s,k}^{[\iota]})^T P_s \alpha_s \mathbf{e}_{s,k}^{[\iota]}\Big]. \tag{3.26}$$

Furthermore, in accordance with [7, Eq (22)], it holds that

$$\mathbb{E}\sum_{s=1}^{m}\sum_{\iota=1}^{\aleph-1}(\vec{\mathbf{e}}_{s,k}^{[\iota]})^T \Lambda_s \vec{\mathbf{e}}_{s,k}^{[\iota]} \leq \frac{\aleph\hbar^2}{4\sin^2\frac{\pi}{2\aleph}}\mathbb{E}\sum_{s=1}^{m}\sum_{\iota=1}^{\aleph-1}(\Delta_\iota \mathbf{e}_{s,k}^{[\iota]})^T \Lambda_s \Delta_\iota \mathbf{e}_{s,k}^{[\iota]}, \quad \forall k \in \mathbb{Z}_0. \tag{3.27}$$

3.4. Mean-square exponential cluster synchronization

For $(\iota, k) \in [0, \aleph]_{\mathbb{Z}} \times \mathbb{Z}_0$ and $s = 1, 2, \ldots, m$, introduce the augmented vector

$$\upsilon_{s,k}^{[\iota]} = (\mathbf{e}_{s,k}^{[\iota]}, \Delta \mathbf{e}_{s,k}^{[\iota]}, \Delta_\iota \mathbf{e}_{s,k}^{[\iota]}, \vec{\mathbf{e}}_{s,k}^{[\iota]}).$$

Suppose that Condition $(CI)_3$ is satisfied and that $0 < \varsigma < 1/(1 + \delta_\infty)$. Combining (3.18) with the inequalities derived in Subsection 3.2 and Subsection 3.3, one obtains

$$\mathbb{E}(\Delta V_k) + \varsigma\mathbb{E}(V_k) \leq \mathbb{E}\sum_{s=1}^{m}\sum_{\iota=1}^{\aleph-1}\upsilon_{s,k}^{[\iota]}\underbrace{\begin{pmatrix} \Bbbk_s^{11} & \Bbbk_s^{12} & 0 & \Bbbk_s^{14} \\ * & \Bbbk_s^{22} & 0 & 0 \\ * & * & \Bbbk_s^{33} & 0 \\ * & * & * & \Bbbk_s^{44} \end{pmatrix}}_{\Bbbk_s}(\upsilon_{s,k}^{[\iota]})^T - (1 - \varsigma - \delta_\infty\varsigma)\mathbb{E}(V_{3,k} + V_{4,k})$$

$$\leq \mathbb{E}\sum_{s=1}^{m}\sum_{\iota=1}^{\aleph-1} \upsilon_{s,k}^{[\iota]}\mathbb{k}_s(\upsilon_{s,k}^{[\iota]})^T, \quad \text{when } k \in [n\theta, n\theta+\beta)_{\mathbb{Z}}, \forall n \in \mathbb{Z}_0, \tag{3.28}$$

where

$$\mathbb{k}_s^{11} = (1+\varepsilon)d_s^2\tilde{b}_s^2 P_s + \delta_\infty(\delta_\infty+2)\mathscr{L}_s^f W_s \mathscr{L}_s^f + \frac{m\delta_\infty(\delta_\infty+2)}{h}Y_s - \frac{2}{\hbar}\alpha_s d_s^2\tilde{\gamma}_s\tilde{b}_s P_s + \varsigma\lambda_P P_s,$$

$$\mathbb{k}_s^{22} = ((1+2\varepsilon)\alpha_s^2 + 2\alpha_s + 2\xi + \lambda_P + \varsigma)P_s,$$

$$\mathbb{k}_s^{33} = d_s^2[(1+\varepsilon+\varepsilon^{-1}+\xi^{-1})\aleph_*\tilde{\gamma}_s^2 + 2\tilde{\gamma}_s\tilde{b}_s]P_s + \frac{\aleph\hbar^2}{4\sin^2\frac{\pi}{2\aleph}}\Lambda_s,$$

$$\mathbb{k}_s^{44} = -\Lambda_s, \quad \mathbb{k}_s^{12} = -2(1+\alpha_s)d_s\tilde{b}_s P_s + 2\lambda_P P_s, \quad \mathbb{k}_s^{14} = -\frac{1}{\hbar}\alpha_s d_s^2\tilde{\gamma}_s\tilde{b}_s P_s.$$

If $k \in [n\theta+\beta, n\theta+\theta)_{\mathbb{Z}}$ with $n \in \mathbb{Z}_0$, analogous to (3.28), one obtains

$$\mathbb{E}(\Delta V_k) + \varsigma\mathbb{E}(V_k) \leq \mathbb{E}\sum_{s=1}^{m}\sum_{\iota=1}^{\aleph-1} \upsilon_{s,k}^{[\iota]}\tilde{\mathbb{k}}_s(\upsilon_{s,k}^{[\iota]})^T, \tag{3.29}$$

where $\tilde{\mathbb{k}}_s$ is equal to $\mathbb{k}_s$ with $\alpha_s = \Lambda_s = 0$, $s = 1, 2, \ldots, m$.

Theorem 3.1. *Suppose that* $0 < \varsigma < 1/(1+\delta_\infty)$ *and that Conditions* $(CI)_1$, $(CI)_2$, *and* $(CI)_3$ *are satisfied. In addition, assume that the following statements hold:*

$(CI)_4$ There exist positive constants $\lambda_P > 0$, $\mu \geq 0$, $\alpha_s \geq 0$, a symmetric matrix $P_s > 0$, and diagonal matrices $W_s, Y_s \geq 0$ such that

$$\mathbb{k}_s := \begin{pmatrix} \mathbb{k}_s^{11} & \mathbb{k}_s^{12} & 0 & \mathbb{k}_s^{14} \\ * & \mathbb{k}_s^{22} & 0 & 0 \\ * & * & \mathbb{k}_s^{33} & 0 \\ * & * & * & \mathbb{k}_s^{44} \end{pmatrix} \leq 0,$$

and

$$\tilde{\mathbb{k}}_s' := \begin{pmatrix} \tilde{\mathbb{k}}_s^{11} & \mathbb{k}_s^{12} & 0 & 0 \\ * & \mathbb{k}_s^{22} & 0 & 0 \\ * & * & 0 & 0 \\ * & * & * & 0 \end{pmatrix} \leq \mu\,\mathrm{diag}(P_s, \lambda_P P_s, 0, 0),$$

where

$$\tilde{\mathbb{k}}_s^{11} = (1+\varepsilon)d_s^2\tilde{b}_s^2 P_s + \delta_\infty(\delta_\infty+2)\mathscr{L}_s^f W_s \mathscr{L}_s^f + \frac{m\delta_\infty(\delta_\infty+2)}{h}Y_s + \varsigma\lambda_P P_s, \quad s = 1, 2, \ldots, m.$$

$(CI)_5$ $\mu_* := \max\left\{(1-\varsigma+\mu)^{\theta-\beta}(1-\varsigma)^{\beta}, (1-\varsigma)^{\beta}\right\} < 1.$

Then, under the intermittent BC law (2.7), System (2.1) achieves m-cluster exponential synchronization in the mean-square sense.

Proof. For $k \in (n\theta, n\theta+\beta]_{\mathbb{Z}}$, $\forall n \in \mathbb{Z}_0$, via (3.28),

$$\mathbb{E}(V_{k+1}) \le (1-\varsigma)\mathbb{E}(V_k) \to \mathbb{E}(V_k) \le (1-\varsigma)^{k-n\theta}\mathbb{E}(V_{n\theta}) \le \mathbb{E}(V_{n\theta}).$$

From (3.29) and $(CI)_4$, we get

$$\mathbb{E}(\Delta V_k) + \varsigma\mathbb{E}(V_k) \le \mathbb{E}\sum_{s=1}^{m}\sum_{\iota=1}^{\aleph-1} \upsilon_{s,k}^{[\iota]}\tilde{\mathbb{K}}_s'(\upsilon_{s,k}^{[\iota]})^T \le \mu\mathbb{E}(V_k) \to \mathbb{E}(V_{k+1}) \le (1-\varsigma+\mu)\mathbb{E}(V_k),$$

which implies

$$\mathbb{E}(V_k) \le (1-\varsigma+\mu)^{k-n\theta-\beta}\mathbb{E}(V_{n\theta+\beta}) \le (1-\varsigma+\mu)^{k-n\theta-\beta}(1-\varsigma)^{\beta}\mathbb{E}(V_{n\theta}) \le \mu_*\mathbb{E}(V_{n\theta}),$$

if $k \in (n\theta+\beta, n\theta+\theta]_{\mathbb{Z}}$ with $n \in \mathbb{Z}_0$. It then becomes apparent that

$$\mathbb{E}(V_{n\theta}) \le \mu_*\mathbb{E}(V_{n\theta-\theta}) \le \cdots \le \mu_*^n\mathbb{E}(V_0) \to 0, \text{ as } n \to \infty.$$

Additionally, $\mathbb{E}(V_k) \le \mathbb{E}(V_{n\theta}) \le \mu_*^n\mathbb{E}(V_0) = \mu_*^{\frac{k}{\theta}-1}\mu_*^{\frac{1}{\theta}(n\theta+\theta-k)}\mathbb{E}(V_0) \le \mu_*^{-1}\mathbb{E}(V_0)\mu_*^{\frac{k}{\theta}}$, where $k \in (n\theta, n\theta+\theta]_{\mathbb{Z}}, n \in \mathbb{Z}_0$. Hence,

$$\lambda_P\underline{\lambda}_P^e\mathbb{E}\sum_{s=1}^{m}\sum_{\iota=1}^{\aleph-1}(\mathbf{e}_{s,k}^{[\iota]})^T\mathbf{e}_{s,k}^{[\iota]} \le \mathbb{E}(V_k) \le \mu_*^{-1}\mathbb{E}(V_0)\mu_*^{\frac{k}{\theta}} \to \mathbb{E}\sum_{s=1}^{m}\sum_{\iota=1}^{\aleph-1}\|\mathbf{e}_{s,k}^{[\iota]}\|^2 \le \frac{\mathbb{E}(V_0)}{\mu_*\lambda_P\underline{\lambda}_P^e}\mu_*^{\frac{k}{\theta}}, \quad \forall k \in \mathbb{Z}_0,$$

where $\underline{\lambda}_P^e$ is the minimum eigenvalue of P_s for all $s = 1, 2, \dots, m$. This completes the proof. □

Remark 3.1. *The scalars $\epsilon > 0$, $\xi > 0$, and $\mu \ge 0$ are free tuning parameters rather than physical parameters of the network. The parameters ϵ and ξ originate from the estimates of cross terms. Because ϵ, ϵ^{-1}, ξ, and ξ^{-1} appear simultaneously in the resulting matrix inequalities, neither excessively small nor excessively large values are generally favorable. In practice, ϵ and ξ can be determined by a coarse-to-fine search over positive values.*

For each fixed pair (ϵ, ξ), the admissible range of μ can first be determined from Condition $(CI)_5$. In particular, for $\beta < \theta$, $(1-\varsigma+\mu)^{\theta-\beta}(1-\varsigma)^{\beta} < 1$ is equivalent to $0 \le \mu < (1-\varsigma)^{-\frac{\beta}{\theta-\beta}} - (1-\varsigma)$. The remaining matrix inequalities can then be tested for feasibility for each candidate value of μ. Notice that a larger μ relaxes the matrix inequality corresponding to the control-off interval, whereas it increases the contraction factor μ^* and hence weakens the predicted convergence rate. Therefore, a convenient practical strategy is to select the smallest μ that renders the matrix inequalities feasible. Among the feasible combinations of (ϵ, ξ, μ), the one with a larger feasibility margin or a smaller μ^* may be preferred.

Corollary 3.1 (Continuous BC case)**.** *Assume that the conditions $(CI)_2$, $(CI)_3$, and $(CI)_4$ in* Theorem 3.1 *hold, and let $0 < \varsigma < 1/(1+\delta_\infty)$. Further, assume that the intermittent control width satisfies $\beta = \theta$; that is, the BC is active throughout each control period. If the corresponding parameter μ^* in $(CI)_5$ (with $\beta = \theta$) satisfies $\mu^* < 1$, then SINN* (2.1) *achieves mean-square exponential m-cluster synchronization under the continuous BC law.*

Proof. The result follows directly from Theorem 3.1 by setting $\beta = \theta$, which eliminates the control-off interval in the intermittent BC scheme. □

Corollary 3.2 (Zero-growth condition during control-off interval)**.** *Assume that the conditions* $(CI)_2$*,* $(CI)_3$*, and* $(CI)_4$ *in* Theorem 3.1 *hold, and let* $0 < \varsigma < 1/(1 + \delta_\infty)$*. If the parameter* μ^* *in* $(CI)_5$ *(with* $\mu = 0$*) satisfies* $\mu^* < 1$*, then SINN* (2.1) *achieves mean-square exponential m-cluster synchronization under the intermittent BC law* (2.7).

Proof. The conclusion is obtained from Theorem 3.1 by choosing $\mu = 0$, which enforces non-expansiveness of the Lyapunov functional during the control-off interval. □

Remark 3.2. *Although [8] and [9] primarily addressed existence, boundedness, exponential stability, and random periodicity, and [7] studied heterogeneous antisynchronization, these works remain essentially within single-objective stability or pairwise synchronization paradigms. The present paper advances the theme to mean-square exponential cluster synchronization under stochastic disturbances, spatial diffusion, and time delays.* Theorem 3.1 *establishes not only convergence of synchronization errors but also an explicit exponential decay rate in the mean-square sense. This represents a conceptual shift from stability analysis of isolated networks to the coordinated organization of clustered stochastic diffusion systems.*

Remark 3.3. *In the existing literature, [8] adopts guaranteed cost control, [7] designs boundary feedback with adaptive corrective laws, and [9] does not involve synchronization control. Overall, most control strategies are continuous or internally applied. The present work proposes an intermittent BC strategy within a clustered structure, where control acts only on boundary nodes during prescribed time intervals and is switched off otherwise. Despite this reduced control duty cycle,* Theorem 3.1 *shows that mean-square exponential synchronization is still guaranteed via LMI-type conditions. The integration of clustering, boundary-based actuation, and temporal intermittency constitutes a comprehensive enhancement of control design for SINNs.*

4. Numerical example

In this section, a numerical example is provided to verify the effectiveness of the proposed intermittent boundary synchronization scheme for clustered differencing SINNs. A multinode network with a prescribed cluster structure is constructed, where all parameters satisfy the theoretical assumptions. With properly chosen control gains and duty cycle parameters, the synchronization criteria are validated numerically. Simulation results show that, despite inertia, diffusion, stochastic disturbances, and delays, the synchronization errors converge to zero in the mean-square exponential sense, confirming the correctness and feasibility of the proposed method. The verification framework adopted in this section is illustrated in Figure 1.

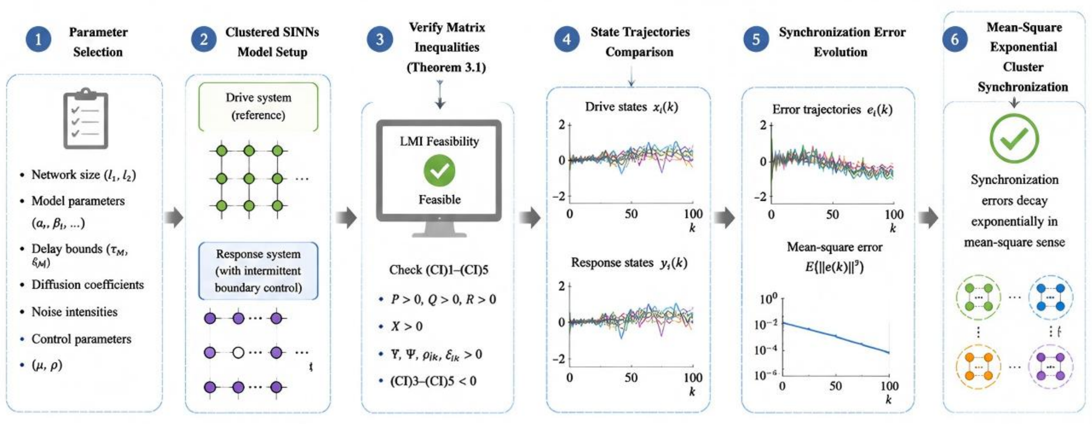

Figure 1. Verification framework of the numerical example.

Consider the two-cluster drive INN:

$$\begin{aligned}\Delta^2 z_{i,k}^{[\iota]} &= 2(e^{-\frac{1}{2}a_i h}-1)\Delta z_{i,k}^{[\iota]} + \left[\frac{2-2e^{-\frac{1}{2}a_i h}}{a_i}\right]^2 \Big[\gamma_i \Delta_\iota^2 z_{i,k}^{[\iota-1]} - b_i z_{i,k}^{[\iota]} \\ &\quad + \sum_{j=1}^{n} c f_j(z_{j,k}^{[\iota]}) + \frac{1}{\sqrt{h}}\sum_{j=1}^{n} \xi\sigma_j(z_{j,k-2}^{[\iota]})\varepsilon_{j,k} + I_i\Big], \quad \forall \iota \in (0,5)_{\mathbb{Z}}, \end{aligned} \tag{4.1}$$

where $i = 1,2,3$, $f_1(s) = f_2(s) = \sin(s)$, $f_3(s) = \cos(s)$, $\sigma_1(s) = \sigma_2(s) = \cos(s)$, $\sigma_3(s) = \sin(s)$, $a_1 = a_2 = 30, a_3 = 35, h = 0.01, \hbar = 0.05$, $\gamma_1 = \gamma_2 = -0.001, \gamma_3 = -0.002, b_1 = b_2 = 10, b_3 = 10.5, c = 0.001, \xi = 0.002, I_1 = I_2 = 20, I_3 = -10$. The two clusters are assigned the boundary control gains $\alpha_1 = -5$ and $\alpha_2 = -4$, respectively; equivalently, the neuronwise gains used in the simulation are -5 for $i = 1,2$ and -4 for $i = 3$. The initial and boundary values are depicted as

$$z_{i,\tau}^{[\iota]} = 1, \quad \forall \tau \in [-2,1]_{\mathbb{Z}}, \iota \in (0,5)_{\mathbb{Z}}; \quad z_{i,k}^{[0]} = 0 = \Delta_\iota z_{i,k}^{[4]}, \quad \forall k \in \mathbb{Z}_0, i = 1,2,3.$$

As noted in Section 2, the response two-cluster INN is governed by

$$\begin{cases} \Delta^2 w_{i,k}^{[\iota]} = 2(e^{-\frac{1}{2}a_i h}-1)\Delta w_{i,k}^{[\iota]} + \left[\frac{2-2e^{-\frac{1}{2}a_i h}}{a_i}\right]^2 \Big[\gamma_i \Delta_\iota^2 w_{i,k}^{[\iota-1]} - b_i w_{i,k}^{[\iota]} \\ \qquad + \sum_{j=1}^{n} c f_j(w_{j,k}^{[\iota]}) + \frac{1}{\sqrt{h}}\sum_{j=1}^{n} \xi\sigma_j(w_{j,k-2}^{[\iota]})\varepsilon_{j,k} + I_i\Big], \quad \forall \iota \in (0,5)_{\mathbb{Z}}, \\ w_{i,\tau}^{[\iota]} = -1, \quad \forall \tau \in [-2,1]_{\mathbb{Z}}, \iota \in (0,5)_{\mathbb{Z}}; \quad w_{i,k}^{[0]} = 0, \ \Delta_\iota w_{i,k}^{[4]} = \rho_{i,k}, \end{cases} \tag{4.2}$$

where $k \in \mathbb{Z}_0$, $i = 1,2,3$; ρ_i denotes the intermittent control input:

$$\rho_{i,k} = \begin{cases} \alpha_i \sum_{\iota=1}^{\aleph-1} (w_{i,k}^{[\iota]} - z_{i,k}^{[\iota]}), & \text{if } k \in [6n, 6n+2)_{\mathbb{Z}}; \\ 0, & \text{if } k \in [6n+2, 6n+6)_{\mathbb{Z}}, n \in \mathbb{Z}_0, \end{cases} \tag{4.3}$$

where $i = 1,2,3$.

Clearly, $\delta_\infty = 2$, $m = 2$, $\theta = 6$, and $\beta = 2$. Taking $\mu = \varsigma = \xi = \epsilon = 0.1$, $\lambda_P = 10^{-4}$, $P_s = \text{diag}(1, 2)$, $\Lambda_s = 10^{-9}$, $W_s = 10^{-5}$, and $Y_s = 10^{-9}$, $s = 1, 2$, the matrix inequalities in $(CI)_3$ and $(CI)_4$ are numerically verified to be feasible. Moreover,

$$\begin{aligned}\mu^* &= \max\left\{(1-\varsigma+\mu)^{\theta-\beta}(1-\varsigma)^\beta, (1-\varsigma)^\beta\right\}\\ &= \max\left\{(1-0.1+0.1)^4(1-0.1)^2,\ (1-0.1)^2\right\} = 0.81 < 1,\end{aligned}$$

and hence, Condition $(CI)_5$ is also satisfied. Conditions $(CI)_1$ and $(CI)_2$ follow directly from the cluster parameters and the Lipschitz properties of the selected activation functions. Therefore, all the conditions of Theorem 3.1 are fulfilled, and Systems (4.1) and (4.2) achieve mean-square exponential cluster synchronization under the intermittent boundary control law (4.3).

Figures 2–7 provide a spatially resolved verification of cluster synchronization under intermittent boundary control by presenting the time evolutions at three distinct spatial nodes $\iota = 1, 3, 5$. Figures 2–4 display the state trajectories of the drive system $z^{[\iota]}_{i,k}$ and the response system $w^{[\iota]}_{i,k}$ at $\iota = 1, 3, 5$, respectively, for $i = 1, 2, 3$. At $\iota = 1$ (Figure 2) and $\iota = 3$ (Figure 3), the response trajectories initially deviate significantly from the drive trajectories due to different initial conditions, but they gradually approach and eventually overlap with them as k increases, indicating successful tracking under boundary control. At $\iota = 5$ (Figure 4), which is closer to the controlled boundary, noticeable high-frequency oscillations appear in the early stage of the response states due to stochastic disturbance and boundary actuation; however, these oscillations are progressively attenuated, and the trajectories ultimately coincide with the drive states. This spatial comparison reveals that synchronization propagates from the controlled boundary into the interior domain.

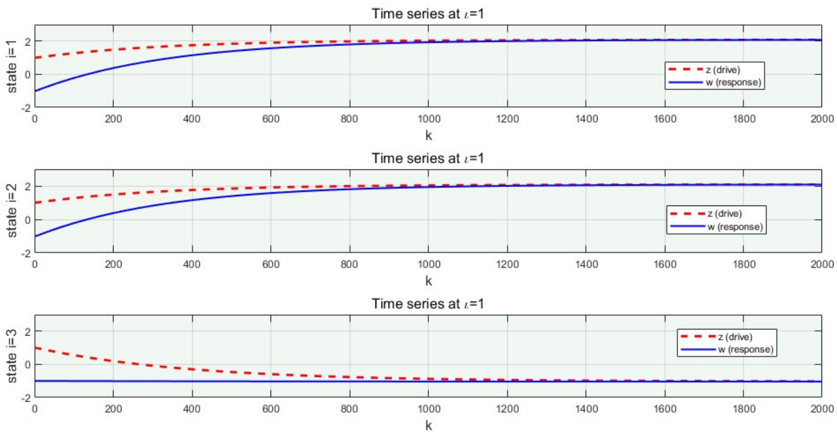

Figure 2. The state trajectories: $w^{[1]}_{i,k}, z^{[1]}_{i,k}$, $i = 1, 2, 3$.

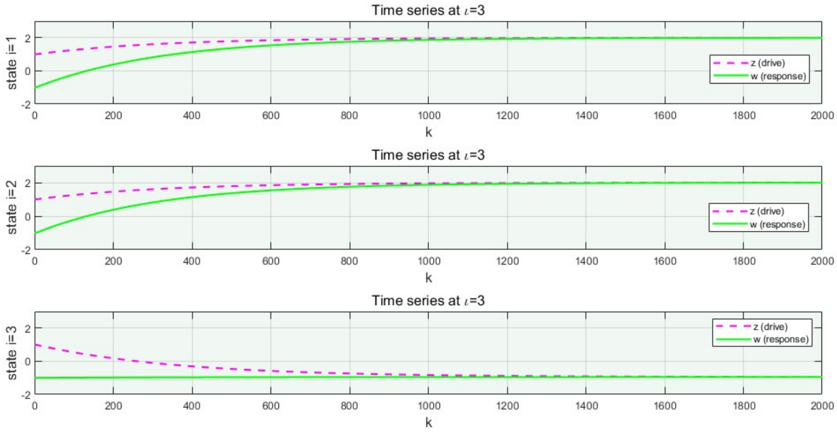

Figure 3. The state trajectories: $w_{i,k}^{[3]}, z_{i,k}^{[3]}$, $i = 1, 2, 3$.

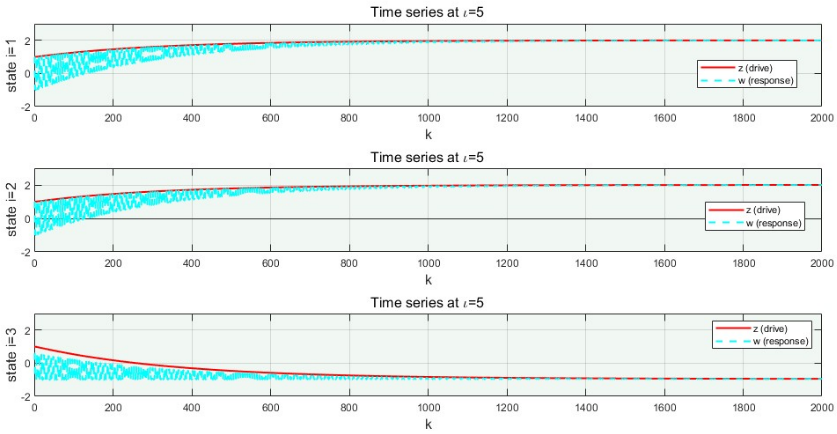

Figure 4. The state trajectories: $w_{i,k}^{[5]}, z_{i,k}^{[5]}$, $i = 1, 2, 3$.

Figures 5–7 further quantify synchronization by plotting the errors $w_{i,k}^{[\iota]} - z_{i,k}^{[\iota]}$ at the same spatial nodes. At $\iota = 1$ (Figure 5) and $\iota = 3$ (Figure 6), the errors exhibit a smooth, monotonic decay toward zero, reflecting exponential convergence in mean-square sense. At $\iota = 5$ (Figure 7), the error shows pronounced oscillatory fluctuations at early times due to the direct influence of boundary control and stochastic excitation, yet its amplitude decays exponentially and eventually vanishes. Collectively, these figures imply that intermittent boundary control is capable of overcoming inertia, diffusion, and stochastic perturbations, and that synchronization is not instantaneous but propagates spatially with transient oscillations near the boundary before achieving global exponential convergence.

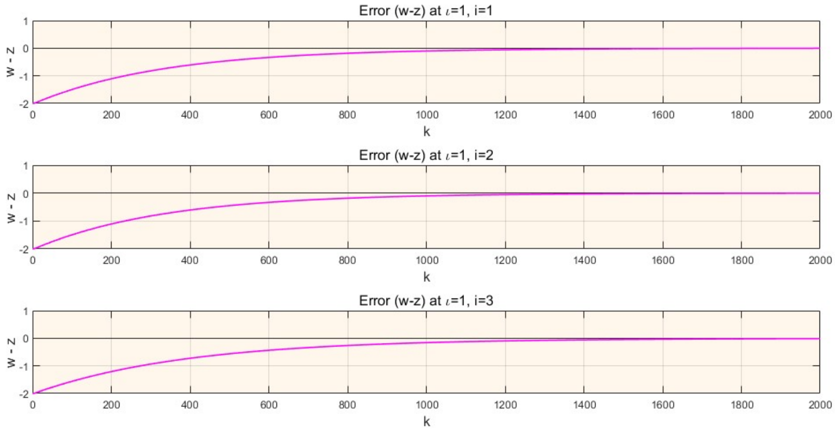

Figure 5. The error trajectories: $w^{[1]}_{i,k} - z^{[1]}_{i,k}$, $i = 1, 2, 3$.

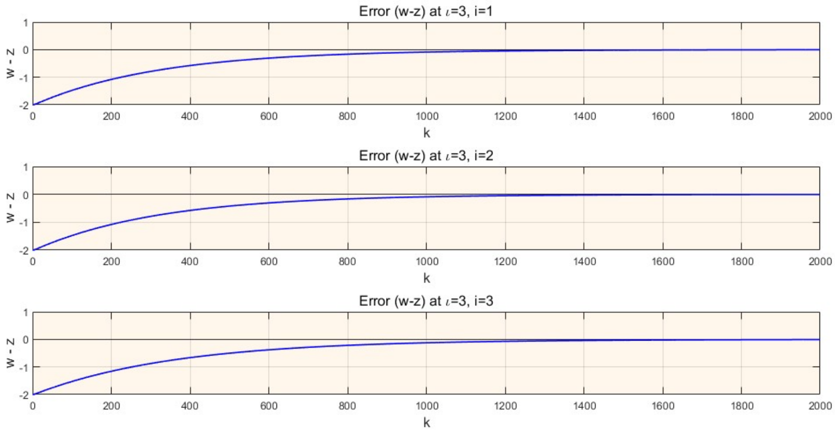

Figure 6. The error trajectories: $w^{[3]}_{i,k} - z^{[3]}_{i,k}$, $i = 1, 2, 3$.

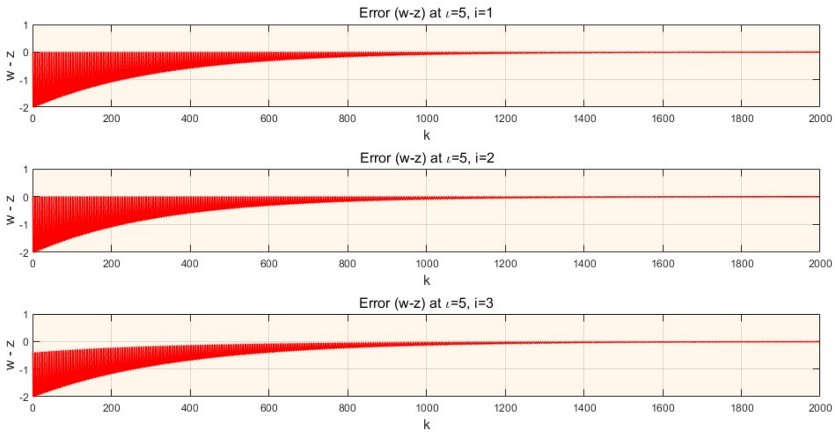

Figure 7. The error trajectories: $w^{[5]}_{i,k} - z^{[5]}_{i,k}$, $i = 1, 2, 3$.

Figures 8–11 examine the robustness of the proposed synchronization scheme under five independent standard normal random initial values for each case. Here, neuron $i = 1$ belongs to the first cluster, whereas neuron $i = 3$ belongs to the second cluster. At the interior node $\iota = 3$ (Figures

8 and 10), both the first-cluster state $z^{[3]}_{1,k}$ and the second-cluster state $z^{[3]}_{3,k}$ (solid lines) together with their corresponding response states $w^{[3]}_{1,k}$ and $w^{[3]}_{3,k}$ (dotted lines) initially display significant dispersion due to different Gaussian initializations, but all trajectories gradually converge, and the response states asymptotically coincide with the drive states. At the boundary-adjacent node $\iota = 5$ (Figures 9 and 11), stronger transient oscillations and larger variability are observed in the early stage, especially because this location is directly influenced by boundary control and stochastic perturbations; nevertheless, both clusters still achieve convergence and trajectory matching as time evolves. These results indicate that synchronization holds for different clusters and spatial locations simultaneously, and that the intermittent boundary control guarantees spatially consistent and clusterwise robust synchronization despite heterogeneous neuron dynamics and multiple independent random initial conditions.

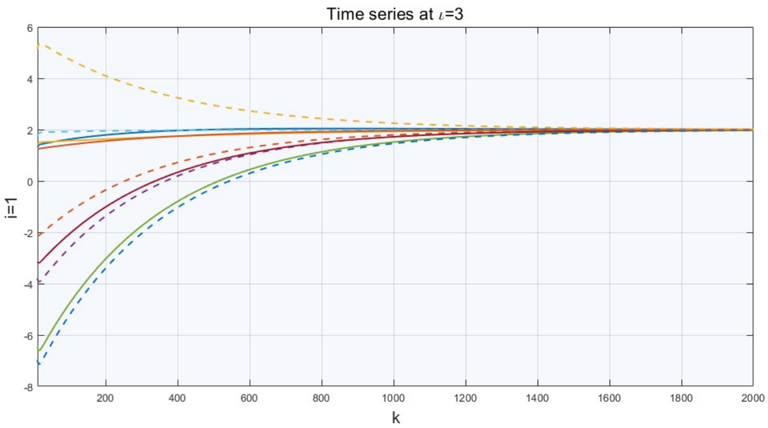

Figure 8. Synchronized robustness under random initial values. Full line: $z^{[3]}_1$; Dotted line: $w^{[3]}_1$.

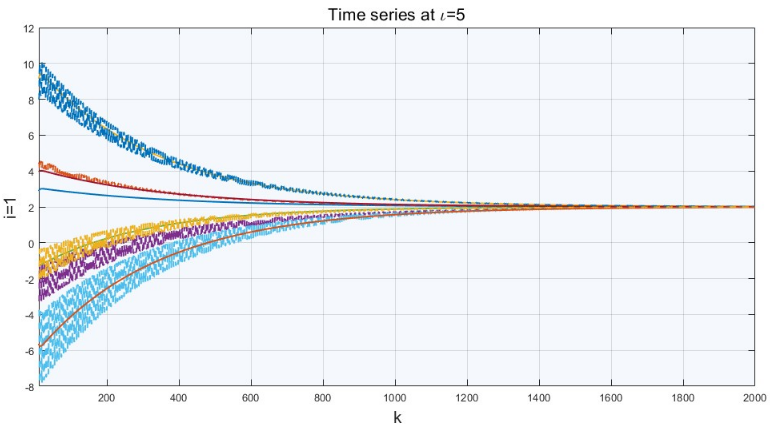

Figure 9. Synchronized robustness under random initial values. Full line: $z^{[5]}_1$; Dotted line: $w^{[5]}_1$.

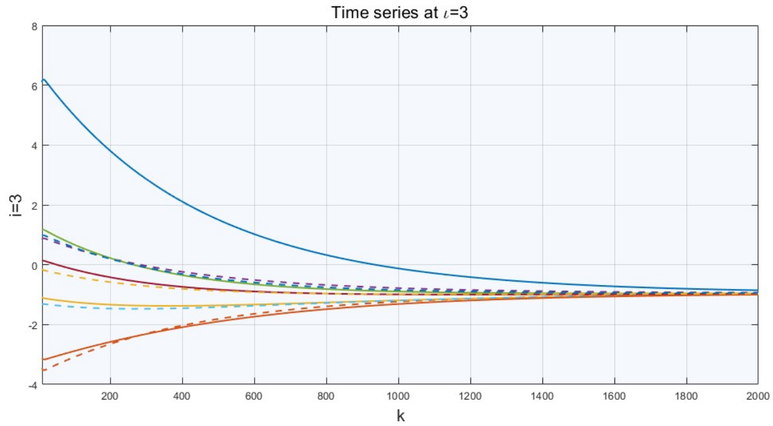

Figure 10. Synchronized robustness under random initial values. Full line: $z_3^{[3]}$; Dotted line: $w_3^{[3]}$.

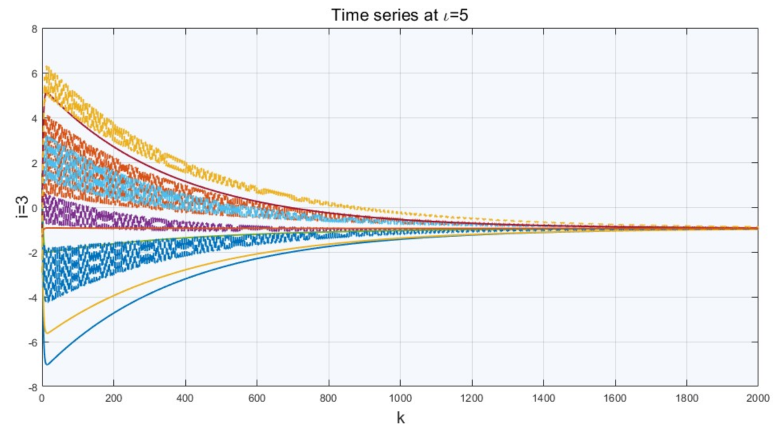

Figure 11. Synchronized robustness under random initial values. Full line: $z_3^{[5]}$; Dotted line: $w_3^{[5]}$.

Figures 12–14 present three-dimensional spatiotemporal surfaces of the drive states $z_{i,k}^{[\iota]}$, the response states $w_{i,k}^{[\iota]}$, and their synchronization errors $w_{i,k}^{[\iota]} - z_{i,k}^{[\iota]}$ for $i = 1, 2, 3$, where the initial values of the drive and response systems are set to 1 and -1, respectively. For each neuron, the left subfigure illustrates the evolution of $z_{i,k}^{[\iota]}$ and $w_{i,k}^{[\iota]}$ over both time k and spatial index ι, showing that although the two systems start from opposite initial states, their surfaces gradually approach and eventually overlap across the entire spatial domain. The right subfigure displays the corresponding error surface, which initially has large magnitude due to the contrasting initial values but decays smoothly toward zero as k increases. The distinction among Figures 12–14 lies in the neuron index: $i = 1$ and $i = 2$ (first cluster) exhibit convergence toward a common positive steady profile, whereas $i = 3$ (second cluster) converges toward a different equilibrium level, reflecting the cluster synchronization structure. Their intrinsic connection is that, for all neurons and all spatial nodes, the error surfaces uniformly collapse to zero, demonstrating global spatiotemporal synchronization despite strongly mismatched initial conditions. These figures imply that the proposed intermittent boundary control not only guarantees exponential error attenuation but also enforces clusterwise coherent behavior throughout the entire spatial domain, confirming robustness against large initial deviations.

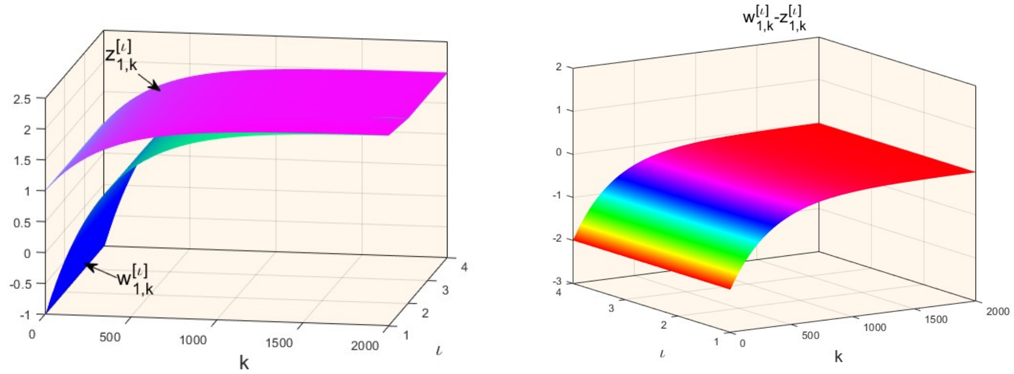

Figure 12. Spatiotemporal surfaces of the drive-response states $z^{[\iota]}_{1,k}$, $w^{[\iota]}_{1,k}$.

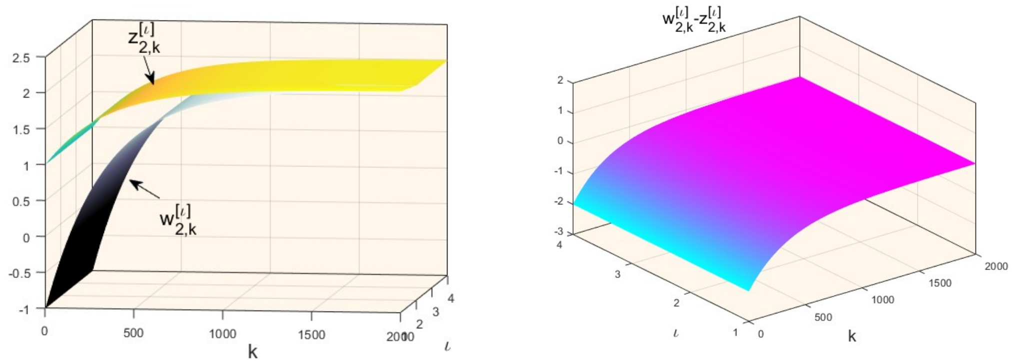

Figure 13. Spatiotemporal surfaces of the drive-response states $z^{[\iota]}_{2,k}$, $w^{[\iota]}_{2,k}$.

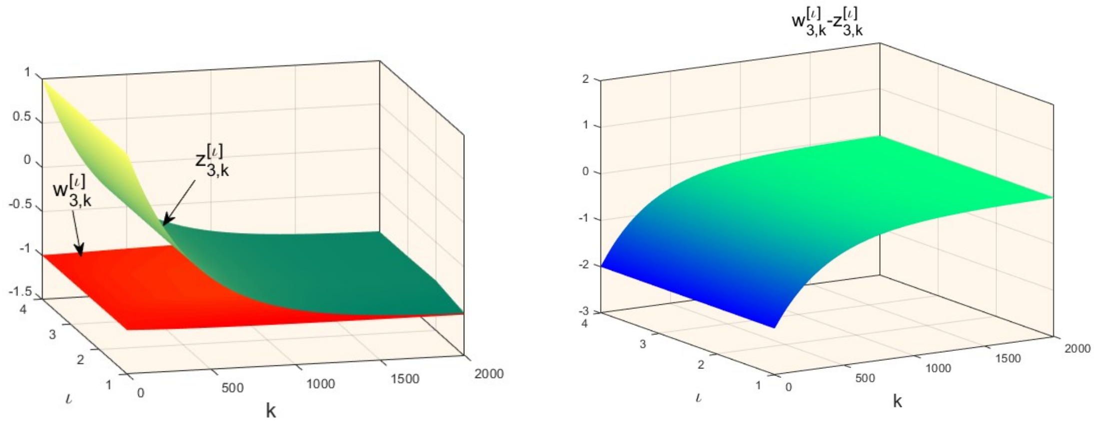

Figure 14. Spatiotemporal surfaces of the drive-response states $z^{[\iota]}_{3,k}$, $w^{[\iota]}_{3,k}$.

5. Conclusions

This paper has addressed the mean-square exponential cluster synchronization problem for a class of clustered discrete space–time stochastic inertial neural networks with diffusion effects and time-varying delays. By incorporating inertial dynamics, spatially discrete diffusion, stochastic perturbations, and dual delay channels into a unified drive–response framework, a control-oriented model has been established for describing cooperative dynamics in stochastic distributed parameter networks.

An energy-efficient intermittent boundary control strategy has been developed to realize cluster synchronization. The proposed controller acts only on boundary nodes and is activated only during prescribed control intervals, which reduces the control activation time compared with continuous boundary actuation. By constructing a six-component discrete Lyapunov–Krasovskii functional and estimating its forward difference over both control-active and control-inactive intervals, sufficient matrix-inequality conditions have been derived to guarantee mean-square exponential cluster synchronization. The obtained criteria explicitly characterize the effects of control gains, duty-cycle parameters, inertial coefficients, diffusion intensities, delay bounds, and stochastic perturbation strengths on the synchronization performance.

A numerical example has been presented to verify the feasibility and effectiveness of the proposed theoretical results. The simulation results show that the designed intermittent boundary controller can ensure the exponential decay of synchronization errors in the mean-square sense, confirming its potential for energy-efficient coordinated control of discrete stochastic diffusion networks.

Future research may focus on extending the proposed framework to more general network topologies, adaptive or event-triggered boundary control schemes, and discrete fractional-order or complex-valued neural network models.

Author contributions

Dong Pan: Conceptualization, Methodology, Formal analysis, Software, Validation, Writing–original draft, Writing–review & editing, Visualization, Project administration; Shaobin Rao: Data curation, Investigation, Software, Supervision, Validation, Writing–review & editing; Weining Li: Funding acquisition, Validation, Writing–review & editing. All authors have read and approved the final version of the manuscript for publication.

Use of Generative-AI tools declaration

The authors declare they have not used Artificial Intelligence (AI) tools in the creation of this article.

Acknowledgments

This work was supported by the 2025 Key Project of Guangxi Social Science Think Tank under Grant No. Zkybkt2025176.

Conflict of interest

The authors declare no conflict of interest.

References

1. G. D. Zhang, J. D. Cao, Aperiodically semi-intermittent-based fixed-time stabilization and synchronization of delayed discontinuous inertial neural networks, *Sci. China Inf. Sci.*, **68** (2025), 112202. http://dx.doi.org/10.1007/s11432-023-4053-9
2. T. N. S. Dongmo, J. Kengne, J. C. Chedjou, Effect of electromagnetic radiations on the dynamics of a five-chain coupled inertial Hopfield neural network and control of multi-stability with the selection of a desired attractor, *Phys. Scr.* , **100** (2025), 015013. http://dx.doi.org/10.1088/1402-4896/ad8e95
3. T. Dong, R. He, H. Q. Li, W. J. Hu, T. W. Huang, Exponential stabilization of phase-change inertial neural networks with time-varying delays, *IEEE T. Syst. Man Cy. Syst.*, **55** (2025), 2659–2669. http://dx.doi.org/10.1109/TSMC.2024.3525038
4. T. Xu, J. E. Zhang, A. L. Wu, Exponential stability of stochastic inertial neural networks with generalised piecewise constant argument, *Int. J. Control*, **98** (2025), 1626–1638. http://dx.doi.org/10.1080/00207179.2024.2417427
5. L. T. Nguyen, A. Eberhard, X. H. Yu, C. J. Li, Accelerating continuous-time optimization with fixed-time time-varying second-order dynamics, *J. Nonlinear Var. Anal.*, **10** (2026), 507–521. http://dx.doi.org/10.23952/jnva.10.2026.3.02
6. Y. X. Jiang, S. Zhu, X. Y. Liu, S. P. Wen, C. X. Mu, Input-to-state stability of delayed memristor-based inertial neural networks via non-reduced order method, *Neural Networks*, **178** (2024), 106545. http://dx.doi.org/10.1016/j.neunet.2024.106545
7. T. W. Zhang, Y. Y. Yang, S. F. Han, Exponential heterogeneous anti-synchronization of multi-variable discrete stochastic inertial neural networks with adaptive corrective parameter, *Eng. Appl. Artif. Intell.*, **142** (2025), 109871. http://dx.doi.org/10.1016/j.engappai.2024.109871
8. T. W. Zhang, H. Z. Qu, Y. T. Liu, J. W. Zhou, Weighted pseudo θ-almost periodic sequence solution and guaranteed cost control for discrete-time and discrete-space stochastic inertial neural networks, *Chaos Soliton. Fract.*, **173** (2023), 113658. http://dx.doi.org/10.1016/j.chaos.2023.113658
9. T. W. Zhang, Y. T. Liu, H. Z. Qu, Global mean-square exponential stability and random periodicity of discrete-time stochastic inertial neural networks with discrete spatial diffusions and Dirichlet boundary condition, *Comput. Math. Appl.*, **141** (2023), 116–128. http://dx.doi.org/10.1016/j.camwa.2023.04.011
10. M. Karamimanesh, E. Abiri, M. Shahsavari, K. Hassanli, A. van Schaik, J. Eshraghian, Spiking neural networks on FPGA: A survey of methodologies and recent advancements, *Neural Networks*, **186** (2025), 107256. http://dx.doi.org/10.1016/j.neunet.2025.107256
11. W. Tian, G. D. Zhang, G. C. Chen, J. H. Hu, S. P. Wen, Fixed-time synchronization of delayed memristive reaction-diffusion neural networks via semi-intermittent switching control, *Appl. Math. Comput.*, **523** (2026), 130026. http://dx.doi.org/10.1016/j.amc.2026.130026
12. M. H. Zhou, Y. J. Li, Y. Y. Cao, X. Y. Ma, Z. T. Xu, Physics-informed spatio-temporal hybrid neural networks for predicting remaining useful life in aircraft engine, *Reliab. Eng. Syst. Safe*, **256** (2025), 110685. http://dx.doi.org/10.1016/j.ress.2024.110685

13. Y. Gholami, Globally asymptotic stability analysis for memristor-based competitive systems of reaction-diffusion delayed neural networks, *Math. Meth. Appl. Sci.*, **46** (2023), 17036–17064. http://dx.doi.org/10.1002/mma.9488

14. H. Y. Tian, Q. X. Zhu, Moment stability of McKean-Vlasov stochastic recurrent neural networks with mixed delays, *Neural Networks*, **196** (2026), 108310. http://dx.doi.org/10.1016/j.neunet.2025.108310

15. D. Chen, K. B. Shi, O. Kwon, X. Cai, Y. B. Sun, S. P. Wen, et al., Fault-tolerant impulsive synchronization in hypercomplex neural networks via AI-driven adaptive switching mechanism, *Commun. Nonlinear Sci.*, **153** (2026), 109511. http://dx.doi.org/10.1016/j.cnsns.2025.109511

16. L. Y. Shi, J. Wang, Decentralized dynamic event-triggered passive bipartite synchronization for semi-Markov jump cooperation-competition neural networks under hybrid random cyber-attacks, *Appl. Math. Comput.*, **507** (2025), 129560. http://dx.doi.org/10.1016/j.amc.2025.129560

17. G. A. Anastassiou, D. Kouloumpou, Brownian motion approximation by neural networks, *Commun. Optim. Theory*, **2023** (2023), 38.

18. J. Rambau, R. Richter, Towards robust adversarial examples for deep neural networks, *J. Appl. Numer. Optim.*, **7** (2025), 291–307. https://dx.doi.org/10.23952/cot.2023.38

19. S. J. M. Burney, Exact solutions of linear multiple delay partial differential equations, *Math. Meth. Appl. Sci.*, **49** (2026), 14282–14291. http://dx.doi.org/10.1002/mma.70732

20. M. S. Siewe, S. Rajasekar, M. Coccolo, M. A. F. Sanjuan, Vibrational resonance in the FitzHugh-Nagumo neuron model under state-dependent time delay, *Chaos*, **35** (2025), 023109. http://dx.doi.org/10.1063/5.0242814

21. N. Manoj, R. Sriraman, Global Mittag-Leffler stability and synchronization of fractional-order Clifford-valued delayed neural networks with reaction-diffusion terms and its application to image encryption, *Inform. Sciences*, **698** (2025), 121773. http://dx.doi.org/10.1016/j.ins.2024.121773

22. L. T. H. Dzung, L. V. Hien, Exponential attractivity of positive inertial neural networks in bidirectional associative memory model with heterogeneous delays, *Comp. Appl. Math.*, **44** (2025), 50. http://dx.doi.org/10.1007/s40314-024-03010-z

23. M. L. Zhu, Y. Zeng, Y. K. Shi, L. G. Wu, H. K. Lam, Extended dissipative analysis for uncertain delayed genetic regulatory networks via interval type-2 T-S fuzzy framework, *IEEE T. Cybernetics*, **56** (2026), 3310–3322. http://dx.doi.org/10.1109/TCYB.2026.3652172

24. L. Yao, Z. Wang, X. Huang, Y. X. Li, Q. Ma, H. Shen, Stochastic sampled-data exponential synchronization of Markovian jump neural networks with time-varying delays, *IEEE T. Neur. Net. Lear.*, **34** (2023), 909–920. http://dx.doi.org/10.1109/TNNLS.2021.3103958

25. W. T. Wang, W. Chen, New study on neutral-type inertial BAM neural networks via the characteristic method, *J. Math. Anal. Appl.*, **557** (2026), 130325. http://dx.doi.org/10.1016/j.jmaa.2025.130325

26. S. Subramaniam, P. Mani, Sampled-data synchronization of Markovian jumping inertial Cohen-Grossberg neural networks with parameter uncertainty and its application in secure communications, *Commun. Nonlinear Sci.*, **156** (2026), 109726. http://dx.doi.org/10.1016/j.cnsns.2026.109726

27. G. Z. Xiang, Z. Yang, Z. Q. Zhang, Asymptotic synchronization of discrete-time BAM neural networks via discrete time Laplace transform, *Expert Syst. Appl.*, **313** (2026), 131537. http://dx.doi.org/10.1016/j.eswa.2026.131537
28. S. Qing, H. M. Wang, S. P. Wen, Fixed/preassigned-time non-chattering synchronization of nonlinear coupled Cohen–Grossberg neural networks via event-triggered control, *Neurocomputing*, **617** (2025), 129069. http://dx.doi.org/10.1016/j.neucom.2024.129069
29. Z. Wang, L. S. Yan, Y. J. Fan, F. Wang, H. Shen, Switching event-triggered-based gain-scheduled control for bipartite synchronization of coupled coopetitive memristive neural networks, *IEEE T. Syst. Man Cy. Syst.*, **55** (2025), 6951–6963. http://dx.doi.org/10.1109/TSMC.2025.3594542
30. Y. Wei, W. Qin, M. Q. Shen, Anti-disturbance synchronization of complex networks with mismatched quantization input via aperiodically intermittent control, *J. Franklin I.*, **363** (2026), 108484. http://dx.doi.org/10.1016/j.jfranklin.2026.108484
31. J. Thomas, E. Steur, C. Fiter, L. Hetel, N. van de Wouw, Exponential synchronization of networked systems under asynchronous sampled-data coupling, *Automatica*, **175** (2025), 112157. http://dx.doi.org/10.1016/j.automatica.2025.112157
32. Z. Wang, X. D. Si, X. Huang, Event-triggered prescribed-time bipartite synchronization of T-S fuzzy coopetition neural networks: A parameters optimizing strategy, *IEEE T. Ind. Inform.*, **22** (2026), 441–451. http://dx.doi.org/10.1109/TII.2025.3611599
33. T. W. Zhang, Z. H. Li, Switching clusters' synchronization for discrete space-time complex dynamical networks via boundary feedback controls, *Pattern Recogn.*, **143** (2023), 109763. http://dx.doi.org/10.1016/j.patcog.2023.109763
34. B. L. Lu, H. J. Jiang, C. Hu, A. Abdurahman, M. Liu, Adaptive pinning cluster synchronization of a stochastic reaction-diffusion complex network, *Neural Networks*, **166** (2023), 524–540. http://dx.doi.org/10.1016/j.neunet.2023.07.034
35. D. Roy, G. V. Rao, *Stochastic dynamics, filtering and optimization*, Cambridge: Cambridge University Press, 2017. http://dx.doi.org/10.1017/9781316863107
36. A. N. Banu, K. Banupriya, R. Krishnasamy, A. Vinodkumar, Robust stability of uncertain stochastic switched inertial neural networks with time-varying delay using state-dependent switching law, *Math. Method. Appl. Sci.*, **46** (2023), 13155–13175. http://dx.doi.org/10.1002/mma.9241
37. P. F. Wang, E. Fridman, Sampled-data finite-dimensional boundary control of 2-D semilinear parabolic stochastic PDEs, *IEEE T. Autom. Control*, **70** (2025), 3456–3463. http://dx.doi.org/10.1109/TAC.2024.3514520
38. K. M. Mohammad, M. Kamrujjaman, Stochastic differential equations to model influenza transmission with continuous and discrete-time Markov chains, *Alex. Eng. J.*, **110** (2025), 329–345. http://dx.doi.org/10.1016/j.aej.2024.10.012
39. T. W. Zhang, Y. K. Li, J. W. Zhou, Data-driven Takagi-Sugeno fuzzy modeling for intermittent black-box complex network synchronization via partial nodes: An application to China's residential housing market, *Expert Syst. Appl.*, **328** (2026), 132687. http://dx.doi.org/10.1016/j.eswa.2026.132687

40. C. Aouiti, H. Jallouli, Exponential stability of pseudo asymptotically ω-periodic solution for delayed Cohen-Grossberg neural networks with double measure, *Int. J. Comput. Math.*, **103** (2026), 199–224. http://dx.doi.org/10.1080/00207160.2025.2546908

41. P. Durairaj, S. Shanmugam, P. Durairaj, M. Rhaima, Bifurcation delay in a network of nonlocally coupled slow-fast FitzHugh–Nagumo neurons, *Eur. Phys. J. B*, **97** (2024), 62. http://dx.doi.org/10.1140/epjb/s10051-024-00707-2

42. T. W. Zhang, S. F. Han, Clustered stochastic gene circuits in dual-node heterogeneous systems: Adaptive learning strategies under a discrete spatio-temporal framework, *Inform. Sciences*, **748** (2026), 123499. http://dx.doi.org/10.1016/j.ins.2026.123499

43. Y. L. Wang, W. H. Chen, S. N. Niu, X. Y. Lu, Stabilization of delayed stochastic reaction-diffusion Cohen-Grossberg neural networks via variable gain intermittent boundary control, *Neural Networks*, **193** (2026), 108041. http://dx.doi.org/10.1016/j.neunet.2025.108041

44. S. B. Rao, X. J. Lv, Passivity-based control and asymptotic synchronization for multi-variable discrete stochastic genetic regulatory networks with complex network dynamics, *Eur. Phys. J. Plus*, **139** (2024), 76. http://dx.doi.org/10.1140/epjp/s13360-024-04860-6